JOURNAL OF Materials CHEMISTRY

Design, synthesis, and characterization of prototypical multistate counters in three distinct architectures†

Karl-Heinz Schweikart,[a] Vladimir L. Malinovskii,[a] James R. Diers,[b] Amir A. Yasseri,[b] David F. Bocian,*[b] Werner G. Kuhr*[b] and Jonathan S. Lindsey*[a]

[a]*Department of Chemistry, North Carolina State University, Raleigh, North Carolina, 27695-8204, USA. E-mail: jlindsey@ncsu.edu*
[b]*Department of Chemistry, University of California, Riverside, California, 92521-0403, USA. E-mail: david.bocian@ucr.edu; werner.kuhr@ucr.edu*

Received 20th September 2001, Accepted 3rd January 2002
First published as an Advance Article on the web 25th February 2002

The storage of multiple bits of information in distinct molecular oxidation states is anticipated to afford extraordinarily high memory densities. Among redox-active molecules, lanthanide porphyrinic triple-decker complexes are attractive candidates for such molecular information storage elements because they provide at least four cationic states over a modest potential range. Our approach toward a molecular multistate counter involves covalently linking two triple deckers with interleaving oxidation potentials to achieve a commensurate increase in the number of oxidation states within a single dyad. We report the design and synthesis of five dyads comprised of triple-decker complexes of the form (Pc)Ln(Pc)Ln(Por) or (Por[1])Ln(Pc)Ln(Por[2]), where Pc = phthalocyaninato, Por = porphyrinato, and Ln = Ce or Eu. The dyads were prepared in a modular building-block fashion by Pd-mediated coupling of an iodophenyl-triple decker and an ethynylphenyl-triple decker. The different dyad architectures examined include a vertical architecture with one linker (V1), a horizontal architecture with one linker (H1), and a horizontal architecture with two linkers (H2). In each dyad, one or two *S*-acetylthiomethyl groups incorporated on the porphyrinic moiety of the triple decker enables attachment to an electroactive surface *via in situ* cleavage of the protected thiol linker(s). Three dyads (**Dyad1–3**) have the V1 architecture but different compositions of triple deckers; three dyads (**Dyad3–5**) have identical composition but different architectures (V1, H1, H2) for comparison of the properties in self-assembled monolayers (SAMs) on gold. The SAM of each dyad exhibits robust reversible electrochemical behavior; the redox waves are essentially the sum of the waves of the component triple deckers. In contrast, mixtures of the component triple decker monomers form poor quality SAMs with inferior electrochemical characteristics. Accordingly, all three dyad architectures are viable constructs for assembling a multistate counter.

Introduction

Our groups have been investigating how multiple bits of information can be stored at the molecular level.[1–7] Our approach toward molecular-based information storage utilizes the distinct redox states of molecules. Information can be stored either in cationic or anionic states; however, we have chosen to work with molecules that afford a rich set of cationic (rather than anionic) states, owing to their greater stability under real-world (*e.g.*, oxidizing) conditions. One of the principal goals of our research program is to design molecular systems that have a large number of resolvable oxidation states whose potentials are less than 2 V. In addition to storing multiple bits of information, our approach has attributes that include (1) electrical writing/reading, (2) no moving parts, (3) low power consumption, (4) scalability to molecular dimensions, (5) operation under ambient conditions, and (6) retention of stored charge for many minutes after removal of applied potential.

In our prior investigations of multibit information storage, we have employed thiol-functionalized porphyrins,[2–4] ferrocenes,[5] and porphyrinic lanthanide triple-decker sandwich complexes[6,7] as the redox units prepared as self-assembled monolayers (SAMs) on electroactive surfaces (*e.g.*, gold). Among these different classes of molecules, the triple-decker sandwich complexes[8] have proved particularly attractive for multibit information storage because they typically exhibit at least four oxidation states in the range 0–1.4 V (*vs.* Ag/Ag^+), corresponding to the formation of the mono-, di-, tri-, and tetracations.[7,9] The fact that the triple deckers possess four readily accessible cationic oxidation states provides for counting from one to four (where the neutral state is zero), which enables the storage of two bits of information. A complementary approach employs polynuclear cobalt complexes of polypyridine ligands that afford up to 10 resolvable anionic states in solution over the range of −0.5 to −2.9 V.[10] Another approach employs an FeS cluster in the core of a dendrimer.[11]

One of our objectives was to extend the number of distinct oxidation states from four to eight, thus enabling the storage of three bits of information. In principle this can be achieved by utilizing two different triple deckers with well resolved, interleaved redox potentials. Toward this goal, we prepared a library of triple-decker phthalocyaninato and porphyrinato sandwich complexes of lanthanides (Eu, Ce) to elucidate how different macrocycle substituents influence the redox potentials of the complexes.[6,7] Electron-donating groups attached to the porphyrin and/or phthalocyanine building blocks were

†Electronic supplementary information (ESI) available: ^{1}H NMR and ^{13}C NMR spectra for each dipyrromethane; absorption, LD-MS, and ^{1}H NMR spectra for each porphyrin and each triple decker; absorption and LD-MS spectra for each triple-decker dyad. See http://www.rsc.org/suppdata/jm/b1/b108520d/

 DOI: 10.1039/b108520d

employed to shift the redox potentials to less positive values. Solution electrochemical studies revealed a variety of suitable combinations of triple deckers that provide effective interleaving of oxidation potentials. Several of these triple deckers were then selected for thiol-derivatization and attachment to Au. In general, the triple-decker SAMs were found to exhibit robust, reversible electrochemical behavior.[6] These SAMs also exhibited remarkably high charge-retention times (tens to hundreds of seconds).[7] We then selected various combinations of the thiol-derivatized triple deckers with interleaving oxidation potentials and formed mixed SAMs of these complexes.[7] The success of this approach depends on two criteria: (1) the molecules partition equally onto the surface and (2) the redox waves remain well-resolved and interleaved. Our initial studies indicated that criterion 1 was met, but criterion 2 was not. In particular, the mixed triple-decker SAMs exhibited very poorly resolved redox waves. This behavior is most likely due to the formation of very heterogeneous monolayers owing to the different molecular shapes (because of the different macrocycle substituents) of the two types of triple deckers.

In this paper, we describe an alternative approach aimed at achieving criterion 2 above. In this approach two different triple-deckers are joined in a covalent architecture bearing one or two thiol linkers. The studies reported herein explore triple-decker dyads in three different architectures. In one architecture, the triple deckers are arranged vertically wherein the planes of the macrocycles are anticipated to be (approximately) perpendicular to the plane of the surface. This dyad contains a single thiol linker and is designated V1. In the second and third architectures, the triple deckers are arranged horizontally, again with the planes of the macrocycles anticipated to be (approximately) perpendicular to the plane of the surface. One of these dyads contains a single thiol linker, and is designated H1, whereas the other contains a linker on each of the triple-decker building blocks and is designated H2. The electrochemical properties of the several different dyads were studied in both solution and in SAMs on a Au surface. The studies reveal that the covalently linked dyad SAMs exhibit well-resolved redox features (unlike the mixed triple-decker SAMs) and are excellent candidates for preparing multistate counters.[12]

Results and discussion

1 Overview

Choice of triple-decker constituents for the dyads. Lanthanide triple-decker sandwich complexes of porphyrins and phthalocyanines can be prepared either by statistical[6,9] or by rational[13,14] approaches. The statistical approach generally results in a mixture containing the following three types of triple deckers: (Por)Ln(Pc)Ln(Por) (type a), (Pc)Ln(Por)Ln(Pc) (type b), and (Pc)Ln(Pc)Ln(Por) (type c) (Fig. 1).[7,9,15] Isolation of the desired triple decker from this mixture is typically achieved by chromatography. Rational methods do not yet exist for the synthesis of a wide variety of heteronuclear heteroleptic members of the type a, b, and c complexes. However, two rational methods are available for a limited number of different central metals and porphyrin and phthalocyanine ligands. Type c triple deckers are accessible *via* a procedure analogous to that of Weiss,[13] wherein a double decker[16] (Pc)Eu(Pc) is reacted with a half-sandwich complex (Por)Eu(acac).[14] The latter is formed *in situ* starting from the free base porphyrin and $Eu(acac)_3{\cdot}nH_2O$ in refluxing 1,2,4-trichlorobenzene (bp 214 °C).[17] We recently reported a rational method for the preparation under milder conditions of certain members of type a and type c triple deckers containing Eu or Ce.[14] Treating CeI_3 with $LiN(SiMe_3)_2$ and a free base porphyrin in bis(2-methoxyethyl) ether (bp 162 °C) and reacting the resulting $(Por^1)CeI$ half-sandwich complex the

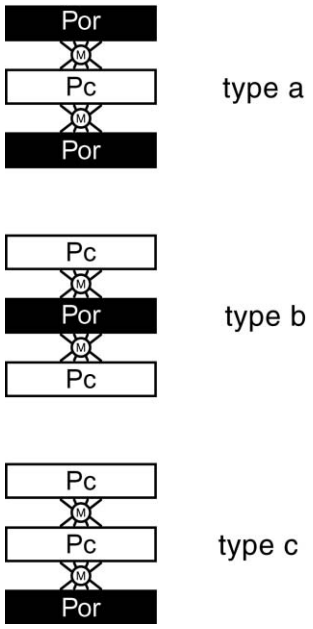

Fig. 1 Schematic structures of the different types of triple deckers.

with double decker[16] $(Por^2)Eu(Pc)$ under reflux affords the mixed type a triple decker $(Por^2)Eu(Pc)Ce(Por^1)$, which is comprised of two different porphyrins (Por^1 and Por^2) and two different metals (Ce and Eu). In the present work, these two rational methods are employed for the synthesis of the type c and type a triple-decker building blocks.

In our previous studies of triple deckers, we identified several classes of complexes as promising candidates for constituents in a multistate counter.[7] A collection of suitable triple deckers of type a or type c, respectively, is presented in Chart 1. Type a triple deckers (**TD1–TD3**) are of form $(TTP)M^1(t\text{-}Bu_4Pc)M^2(Por)$, and type c triple deckers (**TD4–TD6**) are of form $(t\text{-}Bu_4Pc)M^1(t\text{-}Bu_4Pc)M^2(Por)$, where M^1/M^2 = Ce or Eu; $t\text{-}Bu_4PcH_2$ = tetra-*tert*-butylphthalocyanine; $TTPH_2$ = *meso*-tetra-*p*-tolylporphyrin; and $PorH_2$ is a porphyrin bearing *p*-tolyl or *n*-pentyl groups at the *meso*-positions (except for **TD3** which is substituted with a *p*-iodophenyl group and a trimethylsilyl (TMS)-ethynyl group as synthetic handles, and two *p*-tolyl groups). Note that $t\text{-}Bu_4PcH_2$ is composed of a mixture of four regioisomers.[18] We have previously investigated the Eu/Eu triple deckers.[7] The mixed Eu/Ce and Ce/Ce triple deckers are new to this study. The Ce containing complexes were synthesized because additional cationic states are available due to the possibility of metal-centered oxidation(s) (*vide infra*).[19]

The potentials for oxidation of **TD1–TD6** in solution are summarized in Table 1. The data for **TD1**, **TD4**, and **TD6** were taken from ref. 7; the data for **TD2**, **TD3**, and **TD5** were obtained in the present study. Examination of the electrochemical data shows that replacement of one or two Eu by Ce does not lead to a large change in the potentials in most of the cases (*cf.* **TD1** and **TD2**; **TD4** and **TD5**). The largest shift of 0.1 V for $E_{+3/+4}$ is observed for Ce/Ce triple decker **TD2** *vs.* Eu/Eu triple decker **TD1**. However, Ce-containing triple deckers generally exhibit more oxidation waves. Comparison of **TD1** and **TD3** shows that replacement of one Eu by Ce and introduction of synthetic handles (iodophenyl and TMS-ethynylphenyl) to one of the porphyrin rings results in minor shifts of the redox potentials. Considering these observations, we selected three pairs of triple deckers to be combined in dyads (**TD3/TD4**, **TD3/TD6**, and **TD4/TD6**). These combinations were not necessarily chosen to achieve the optimum interleaving of potentials (*i.e.*, to obtain the maximum number of resolved oxidation waves). Instead, certain combinations were

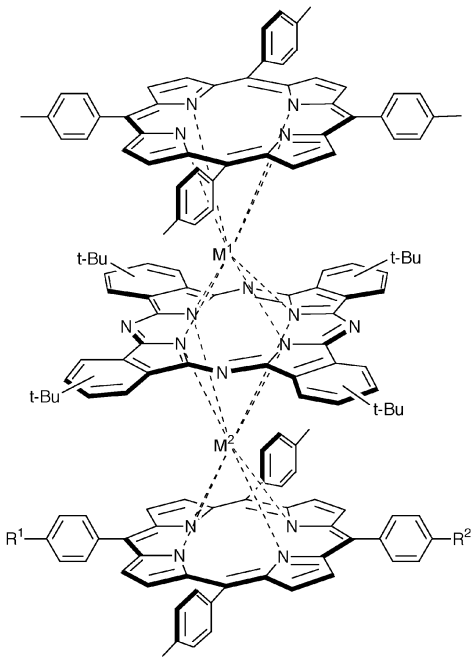

Type a triple deckers

TD1 M^1/M^2 = Eu, R^1/R^2 = CH_3

TD2 M^1/M^2 = Ce, R^1/R^2 = CH_3

TD3 M^1 = Eu, M^2 = Ce, R^1 = I, R^2 = —≡—TMS

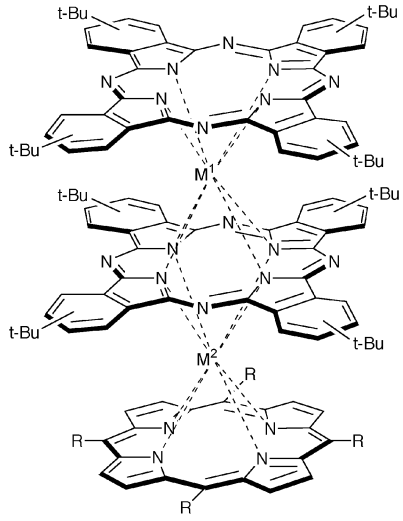

Type c triple deckers

TD4 M^1/M^2 = Eu, R = *p*-tolyl

TD5 M^1 = Eu, M^2 = Ce, R = *p*-tolyl

TD6 M^1/M^2 = Eu, R = *n*-pentyl

Chart 1

chosen to explore how dyad composition might affect SAM quality. For example, the **TD4/TD6** dyad is comprised of two type c triple deckers, whereas the **TD3/TD4** and **TD3/TD6** dyads are each comprised of one type a and one type c triple decker.

Dyad design strategy. The design of a viable multistate counter comprised of two different triple deckers attached to an electroactive surface requires the elucidation of the effects of SAM formation on the redox characteristics of the dyad. In this regard, prior studies of porphyrin arrays revealed that the oxidation potentials of the SAMs are typically shifted

Table 1 Potentials for the oxidation of the benchmark triple deckers in solution[a, b]

Triple decker	Potential/V					
	$E_{0/+1}$	$E_{+1/+2}$	$E_{+2/+3}$	$E_{+3/+4}$	$E_{+4/+5}$	$E_{+5/+6}$
Type a						
TD1	0.26	0.62	0.98	1.27		
TD2	0.26	0.67	0.93	1.17	1.42	1.70
TD3	0.24	0.64	1.00	1.24	1.48	1.68
Type c						
TD4	0.13	0.56	1.01			
TD5	0.06	0.57	1.01	1.25	1.60	
TD6	0.09	0.45	0.89	1.26		

[a]Data for **TD1**, **TD4**, **TD6**, from ref. 7; data for **TD2**, **TD3**, **TD5**, this work. [b]Obtained in BuCN (**TD1**, **TD4**, **TD6**) or CH_2Cl_2 (**TD2**, **TD3**, **TD5**) containing 0.1 M Bu_4NPF_6. *E*-values *vs.* Ag/Ag^+; $FeCp_2/FeCp_2^+$ = 0.19 V; scan rate = 0.1 V s^{-1}. Values are ±0.03 V.

0.05–0.15 V more positive compared with those in solution.[2–4] The exact magnitude of the shift appears to depend on the packing in the SAM. In addition, in large arrays, the potential shift for a porphyrin closer to the surface appears to be slightly larger than that for a porphyrin further from the surface. The extent of these effects in the triple-decker dyads was unknown at the outset of this study and was found to be dependent on the exact composition of the dyad (*vide infra*).

The first design consideration for a multistate counter composed of two triple deckers is whether the dyad should be constituted in a vertical architecture with one linker (V1) or a horizontal architecture with one (H1) or two (H2) linkers, as shown in Fig. 2. The vertical architecture affords the maximum number of molecules per unit area (presuming the two triple deckers are in registry) and could thereby increase functional features such as information-storage density. However, the diphenylethyne group that joins the two triple deckers permits for torsional rotation about the –C≡C– bond. Torsional

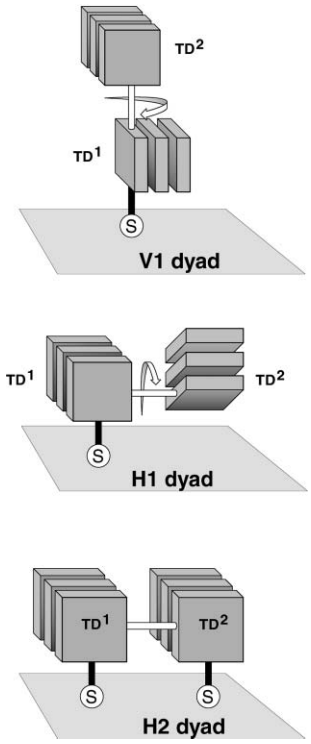

Fig. 2 Schematic structures of the vertical dyad with one linker (V1), horizontal dyad with one linker (H1), and horizontal dyad with two linkers (H2) in self-assembled monolayers (SAMs) attached *via* the thiol linker.

rotation would significantly increase the molecular area. In addition, the two different triple deckers in the V1 architecture are at intrinsically different distances from the electroactive surface. This could be either be advantageous or deleterious for features ranging from redox potential to charge-retention characteristics. The horizontal architecture would occupy an intrinsically larger molecular area on the surface. However, in this design, the two triple deckers should be at similar distances from the surface. Nonetheless, this feature of the H1 dyad could be compromised by torsional rotation of the non-attached triple decker around the –C≡C– bond of the diphenylethyne linker. In contrast, in the case of H2 dyads, both triple deckers are attached to the surface and rotation is suppressed. All three types of architectures were examined herein to determine which design is best for achieving superior SAM formation and redox characteristics.

The next design consideration is the placement of the synthetic handles for joining the triple deckers and for attachment of thiol linkers. These handles can be more easily introduced *via* a suitably functionalized porphyrin rather than a phthalocyanine because the synthetic chemistry of the former class of molecules is better developed.[20] To avoid possible complications due to rotational isomers, we sought only one derivatized porphyrin in each triple decker. In the V1 dyads, the thiol linker is in the *trans* position with respect to the ethyne linker between the two triple deckers, which requires a *trans*-substituted porphyrin (*trans*-A_2BC) bearing the thiol linker. In the H1 and H2 dyads, the thiol linker and the ethyne group are in a *cis* position with respect to each other, which requires a *cis*-substituted porphyrin (*cis*-A_2BC) bearing the thiol linker. Iodophenyl and ethynylphenyl groups attached to the porphyrin constitute suitable handles for Sonogashira coupling of thiol-derivatized linker groups at the triple-decker stage or coupling of the two triple deckers to give the corresponding dyad.

The incorporation of certain types of porphyrin building blocks in triple-decker sandwich complexes can result in a mixture of stereoisomers.[21] Porphyrins of the type A_4, A_3B, *cis*-A_2B_2, *trans*-A_2B_2, and *trans*-A_2BC have at least one mirror plane perpendicular to the plane of the macrocycle. As a result, the formation of a corresponding triple decker affords a single product with a mirror plane perpendicular to the porphyrin and phthalocyanine rings.[22] However, *cis*-A_2BC porphyrins and ABCD porphyrins lack a perpendicular mirror plane and are thus facially enantiotopic. The reaction with a lanthanide metal occurs on one or the other of the two faces of the porphyrin, affording the porphyrin half-sandwich complex as a pair of enantiomers (Fig. 3). The reaction of an appropriate double decker with the enantiomeric half-sandwich complexes gives the corresponding triple decker as a pair of enantiomers.[22] Note that the H1 and H2 dyads, but not the V1 dyads,

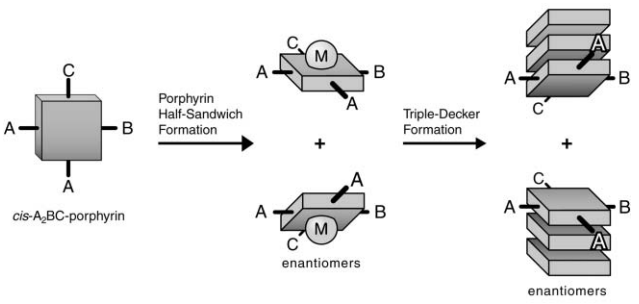

Fig. 3 A *meso*-substituted porphyrin with substituents in a *cis*-A_2BC (or ABCD) pattern is facially enantiotopic. The formation of a half-sandwich complex with a lanthanide metal (M) affords a pair of enantiomers (the ligand on the trivalent metal is omitted for clarity). Subsequent reaction with a lanthanide double decker affords the corresponding triple decker as a pair of enantiomers.[22]

are derived from triple deckers that incorporate a *cis*-A_2BC porphyrin.

The number of isomers grows for dyads comprised of two different triple deckers when one or both incorporates a *cis*-A_2BC porphyrin. For an H1 dyad wherein the triple decker bearing the thiol linker is built around a *cis*-A_2BC porphyrin, the triple decker dyad exists as a pair of enantiomers. For an H2 dyad, both triple deckers incorporate one *cis*-A_2BC porphyrin (Fig. 4). In the latter case, the reaction of the enantiomeric mixture of one triple decker (derived from a *cis*-$A^1{}_2B^1C^1$ porphyrin) and the enantiomeric mixture of a second triple decker (derived from a *cis*-$A^2{}_2B^2C^2$ porphyrin) at the B sites yields the covalently linked triple-decker dyad as four isomers.[22] There are two pairs of *syn*/*anti* stereoisomers, each of which consists of a pair of enantiomers. The terms *syn* and *anti* refer to the positions of the C^1/C^2 substituents with respect to each other. The thiol linker is coupled to the C^1/C^2 sites for attachment of the resulting dyads to an electroactive surface. The *syn* and *anti* isomers have different spatial demands on the surface (Fig. 4), which could potentially compromise the quality of the SAM.[23]

2 Synthesis of triple-decker building blocks and dyads

Porphyrin building blocks. The rational synthesis of porphyrins bearing a distinct pattern of *meso*-substituents begins with dipyrromethanes.[24] Dipyrromethanes bearing aryl substituents at the 5-position are readily available *via* a one-flask synthesis.[25] The 5-aryl dipyrromethanes (**1–3**) employed in this work differ only in the nature of the *p*-aryl substituent (**1** = methyl;[25] **2** = trimethylsilylethynyl;[26] **3** = iodo[25]). Following a general procedure,[27] reaction of dipyrromethane **1** with pyridyl thioester **4**[27] at −78 °C gave the monoacylated dipyrromethane **5** (Scheme 1). Treatment of **5** with EtMgBr followed by acid chloride **6** in tetrahydrofuran (THF) at room temperature afforded **8** in 65% yield. Similar treatment of **5** with 4-iodobenzoyl chloride (**7**) gave **9** in 68% yield. To minimize the amount of free EtMgBr present at any time, EtMgBr (2, 2, 1 equiv) and acid chloride (1, 1, 0.5 equiv) were added sequentially and repeatedly at 5–10 min intervals rather than the entire amount all at once.[27]

The synthesis of the porphyrins proceeds by acid-catalyzed condensation of a dipyrromethane and a dipyrromethane–dicarbinol, followed by oxidation upon addition of 2,3-dichloro-5,6-dicyano-1,4-benzoquinone (DDQ).[24] This method affords the corresponding substituted porphyrin. Using this method, reduction of **8** with $NaBH_4$ followed by condensation of the resulting dicarbinol with dipyrromethane **2** in the presence of trifluoroacetic acid (TFA) (30 mM in acetonitrile) and subsequent oxidation with DDQ at room temperature afforded *cis*-A_2BC porphyrin **11** in 20% yield (Scheme 2). In the same manner, diacyldipyrromethane **9** and dipyrromethane **2** afforded *cis*-A_2BC porphyrin **12**, and diacyldipyrromethane **10**[28] and dipyrromethane **3** gave the A_3B porphyrin **13**, each in 21% yield. Porphyrins **11–13** are key precursors to the corresponding triple-decker building blocks. The porphyrins 5-(4-iodophenyl)-10,20-bis(4-methylphenyl)-15-[4-(2-(trimethylsilyl) ethynyl)phenyl]porphyrin (**14**)[24] and 5-(4-iodophenyl)-10,15, 20-tri-*n*-pentylporphyrin (**15**)[6] have been synthesized previously using the same rational method.

Triple-decker building blocks. The type a and type c triple deckers were prepared following rational synthetic pathways. The synthesis of the type c triple-decker building blocks is shown in Scheme 3. Following a standard method,[13,14] porphyrin **14** was treated with $Eu(acac)_3{\cdot}nH_2O$ and double decker[16] (t-$Bu_4Pc)_2Eu$[14,29] in refluxing 1,2,4-trichlorobenzene (1,2,4-TCB) to afford triple decker **TD7** in 74% yield, bearing one iodophenyl and one TMS-ethyne group. Similarly, triple

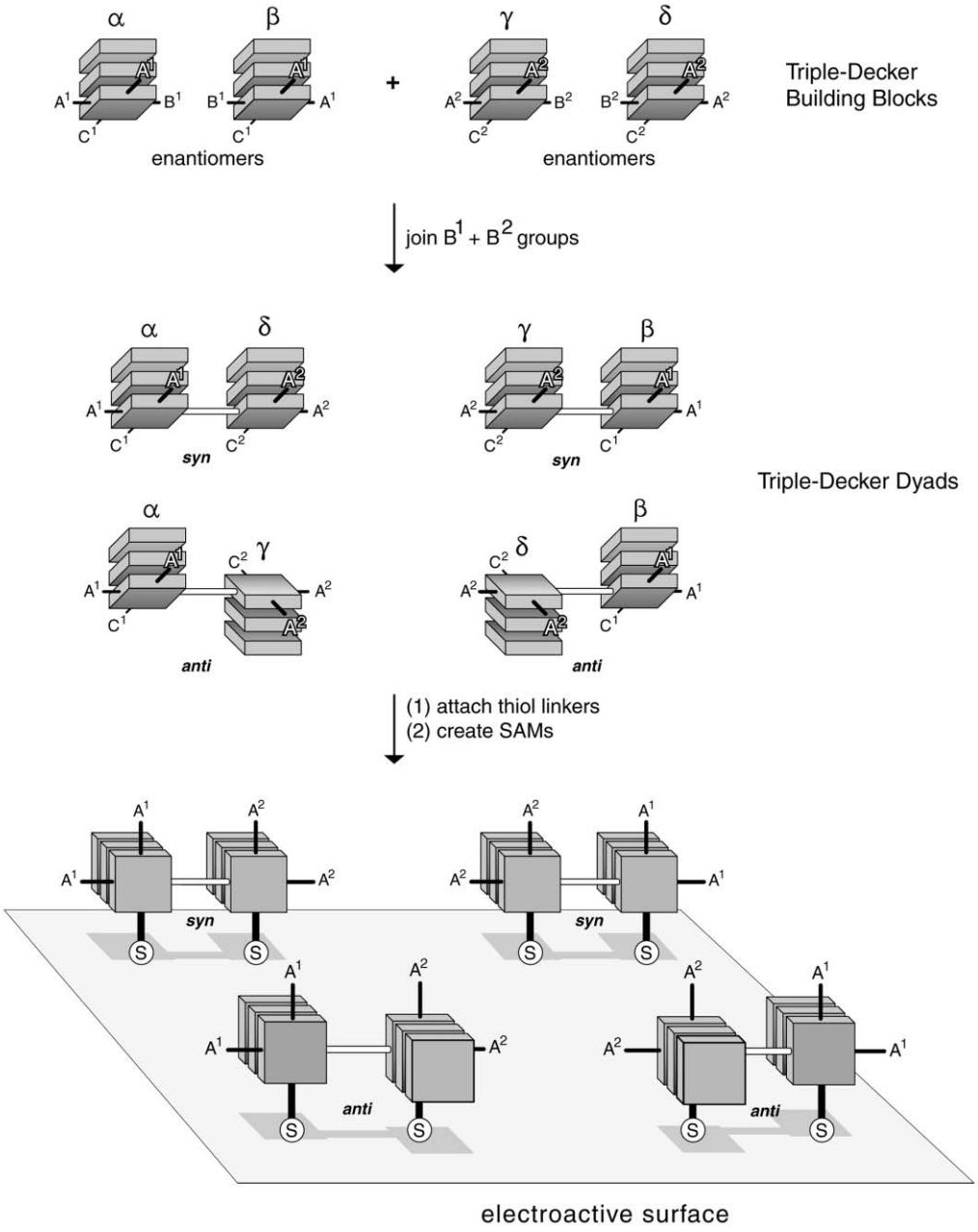

Fig. 4 *syn*/*anti* Stereoisomers of an H2 dyad in a SAM. The coupling of two triple-decker building blocks, each of which comprises a pair of enantiomers, at sites $B^1 + B^2$ (*e.g.*, iodo + ethyne) affords four triple-decker dyads. The four dyads include a pair of *syn* enantiomers and a pair of *anti* enantiomers. Such *syn* and *anti* isomers are expected to pack and orient differently upon attachment to a surface.[23]

deckers **TD8**, **TD9** and **TD10** were obtained in 79%, 62% and 25% yield, respectively, starting from porphyrins **11**, **13** and **15**. Note that in **TD7** the two functional handles are in *trans* configuration, whereas they are in *cis* configuration in **TD8**.

To provide for a free ethyne group in a subsequent Sonogashira-coupling step, the TMS group of triple decker **TD8** was selectively cleaved in the presence of the TIPS group. The cleavage was performed by treating **TD8** with finely powdered K_2CO_3 in a mixture of chloroform, THF, and methanol (1 : 5 : 2) at room temperature, affording ethyne triple decker **TD8′** in 90% yield after chromatography *via* a single silica column (Scheme 4).

Compounds **TD8′** and **TD9** represent the desired functionalized analogues to **TD4** (Chart 1), whereas **TD10** corresponds to **TD6**. The two functional handles (TIPS-ethyne and ethyne) in **TD8′** are *cis* to each other, thereby qualifying **TD8′** as a building block for horizontal dyads (see Fig. 2). The iodophenyl unit in triple deckers **TD9** and **TD10** provides a site for a Sonogashira coupling. Thus, **TD9** and **TD10** will constitute the terminal, non-attached triple-decker units (TD^2) in V1 and H1 dyads.

The synthesis of the type a triple-decker building blocks is shown in Scheme 5. Applying a standard procedure,[14] reaction of porphyrin **12** with CeI_3 and $LiN(SiMe_3)_2$ in refluxing bis(2-methoxyethyl) ether followed by treatment with double decker[16] (*t*-Bu_4Pc)Eu(TTP)[14] afforded **TD11** in 54% yield. In the same manner, **TD3** was resynthesized in 46% yield by reaction of porphyrin **14** with (*t*-Bu_4Pc)Eu(TTP). However, implementation of the reported synthesis[14] of **TD3** failed in three out of five attempts, which prompted us to develop a modified procedure employing stringent avoidance of air and moisture. This refined procedure was applied to the synthesis of **TD11** on three occasions without fail.

Subsequent Sonogashira coupling of **TD11** with 1-[4-(*S*-acetylthiomethyl)phenyl]acetylene (**16**)[2] in a mixture of dry THF and triethylamine (TEA) containing CuI afforded *S*-acetylthiomethyl-substituted triple decker **AcS-TD11** in 57% yield (Scheme 6). In the same manner but using

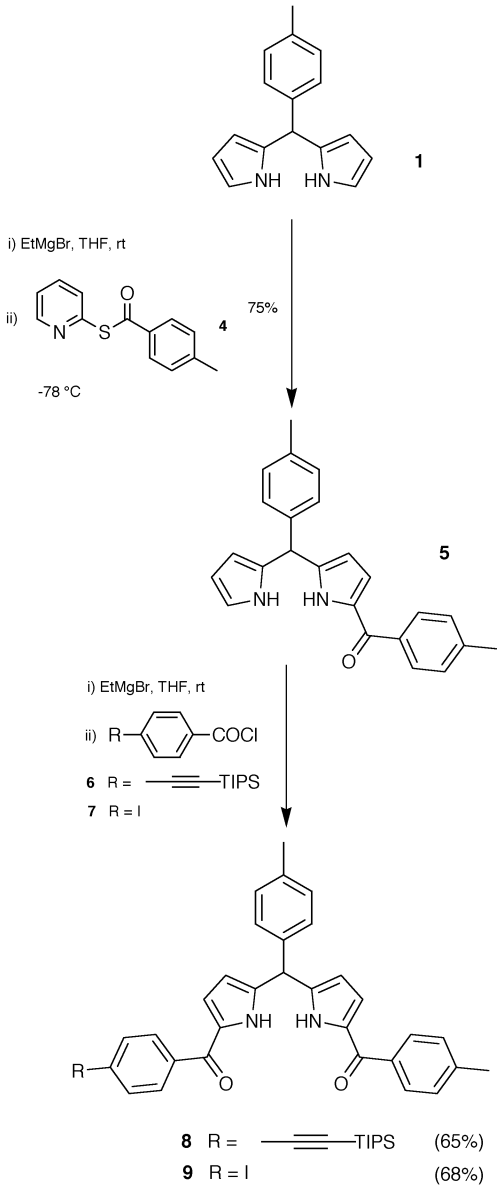

Scheme 1

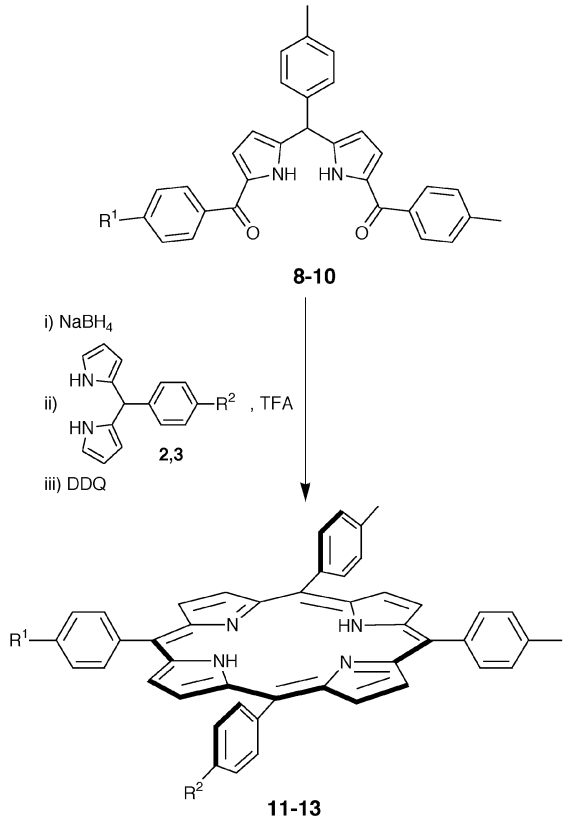

Precursors	R^1	R^2	Porphyrin
8 + **2**	TIPS	TMS	**11** (20%)
9 + **2**	I	TMS	**12** (21%)
10 + **3**	CH_3	I	**13** (21%)

Scheme 2

N,N-diisopropylethylamine (DIEA) instead of TEA, **AcS-TD3** and **AcS-TD7** were obtained in 64% and 59% yield after chromatography, starting from **TD3** and **TD7**, respectively (Schemes 7, 8).

Deprotection of the TMS-ethyne groups of **AcS-TD3**, **AcS-TD7** and **AcS-TD11** with $(n\text{-Bu})_4$NF in THF at 0 °C afforded the desired triple-decker building blocks **AcS-TD3′** (Scheme 7), **AcS-TD7′** (Scheme 8), and **AcS-TD11′** (Scheme 6) in 97%, 89% and 66% yield, respectively. Note that the *S*-acetylthio group and the ethyne group in **AcS-TD11′** are *cis* to each other, whereas they are *trans* in **AcS-TD3′** and **AcS-TD7′**. Thus, **AcS-TD3′** and **AcS-TD7′** will allow the construction of V1 dyads, whereas **AcS-TD11′** is a building block for an H1 dyad (see Fig. 2).

In summary, the triple-decker building blocks were prepared *via* rational synthetic routes. Each triple decker prepared herein exists as a mixture of isomers due to one or both of the following types of substitution of the ligands. (1) The presence of a *cis*-A_2BC porphyrin. A *cis*-A_2BC porphyrin is facially enantiotopic and gives rise to enantiomers of triple deckers (**TD8**, **TD11**, and their derivatives). (2) The presence of one or two tetra-*tert*-butylphthalocyanine ligands. The four regio-isomers of tetra-*tert*-butylphthalocyanine[18] result in a mixture of diastereomers of the triple decker (**TD1**–**TD11** and their derivatives).[30] For packing in SAMs, the isomers of H1 and H2 triple-decker dyads caused by the *cis*-configuration of the porphyrin were anticipated to impose far greater spatial constraints than those caused by different substitution patterns of the *tert*-butyl groups about the perimeter of the phthalocyanine ligands. We first focused on the V1 dyads and decided to prepare a series of three different dyads comprised of monomers with a good interleaving of the oxidation potentials.

Vertical dyads with one linker (V1). The synthesis of **Dyad1** is shown in Scheme 9. *S*-Acetylthio-derivatized ethynylphenyl triple decker **AcS-TD7′** was reacted with iodophenyl triple decker **TD10** in a Sonogashira coupling, applying copper-free reaction conditions [tris(dibenzylideneacetone)dipalladium(0) ($Pd_2(dba)_3$) and tri-*p*-tolylphosphine ($P(o\text{-tol})_3$) in a 5 : 1 mixture of toluene–DIEA at 35 °C] that we have developed for use with porphyrins.[31] A copper-free Pd-catalyzed coupling procedure was employed to avoid homo-coupling of monomer **AcS-TD7′**. The progress of the coupling was monitored by analytical size exclusion chromatography (SEC). Because the reaction proceeded quite slowly, a further batch of catalyst [$Pd_2(dba)_3$ and $P(o\text{-tol})_3$] was added twice during the course of the reaction. After a total elapsed reaction time of 48 h, the SEC trace still showed starting triple-decker monomers (~32%), but also already a considerable amount of oligomeric side products (~26%).[32] Therefore, the reaction was stopped by evaporating the solvent. The desired **Dyad1** was then obtained in 25% yield after a three-column procedure. The

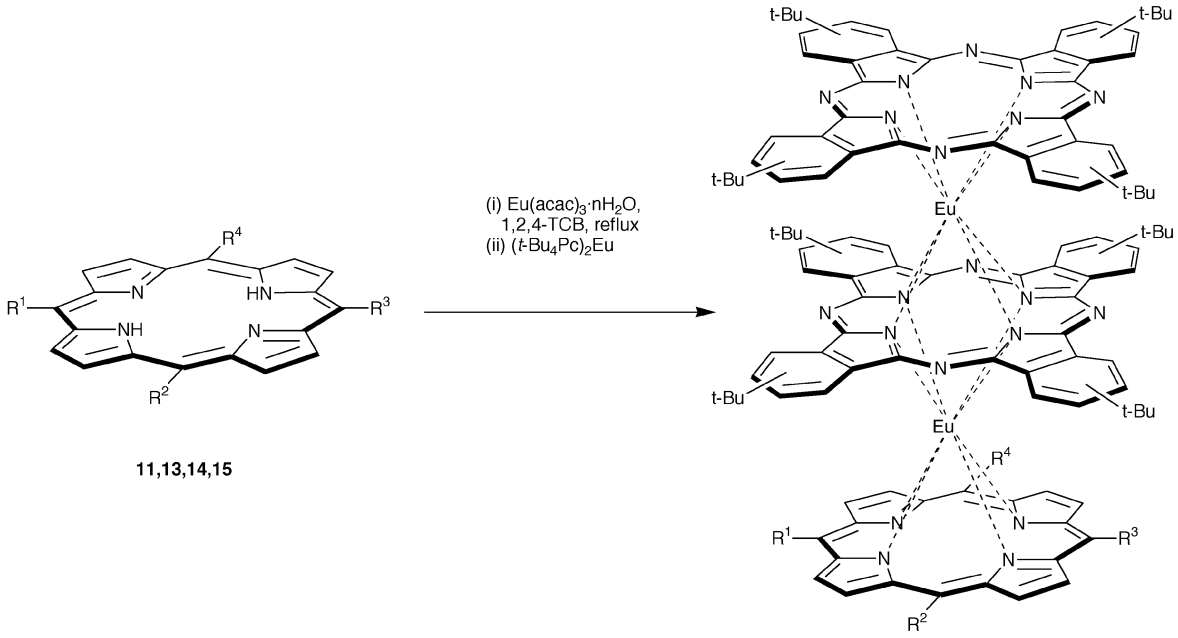

Porphyrin	R^1	R^2	R^3	R^4	Triple Decker	Yield
14	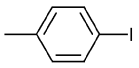	*p*-tolyl	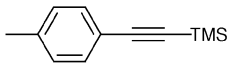	*p*-tolyl	**TD7**	74%
11	*p*-tolyl	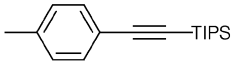	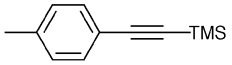	*p*-tolyl	**TD8**	79%
13	*p*-tolyl	*p*-tolyl	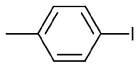	*p*-tolyl	**TD9**	62%
15	*n*-pentyl	*n*-pentyl	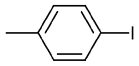	*n*-pentyl	**TD10**	25%

Scheme 3

laser-desorption mass spectrometry (LD-MS) spectrum with the matrix 1,4-bis(5-phenyloxazol-2-yl)benzene (POPOP) showed the molecule ion peak at $m/z = 5001.2$ together with several fragmentation peaks at lower mass.

Analogously, *S*-acetylthio-derivatized triple decker **AcS-TD3′** was treated with **TD10** in a Sonogashira reaction to give **Dyad2** (Scheme 10). Again, further catalyst was added twice, because the reaction had slowed down. Analytical SEC after 21 h revealed that oligomeric side-products had formed (~39%) while unreacted triple-decker monomers (~26%) were still present in the reaction mixture.[32] The reaction was stopped after 24 h, affording **Dyad2** in 25% yield after chromatography. The LD-MS spectrum showed the molecule ion peak at $m/z = 4922.1$, and also a peak at $m/z = 4876.2$ corresponding to fragmentation owing to the cleavage of the *S*-acetylthio group.

The same conditions [$Pd_2(dba)_3$, P(*o*-tol)$_3$ in a 5 : 1 mixture of toluene–DIEA at 35 °C] were applied to the reaction of **AcS-TD3′** and iodophenyl triple decker **TD9** (Scheme 11). The coupling reaction was monitored by analytical SEC, and a further amount of catalyst was added after 20 h. After a total reaction time of 24 h, removal of the solvent and chromatographic work-up afforded **Dyad3** in 51% yield. The LD-MS spectrum (POPOP) showed the molecule ion peak at $m/z = 4979.4$ and a peak at $m/z = 4902.4$ due to cleavage of the *S*-acetylthio linker.

Note that **Dyad2** and **Dyad3** are each comprised of one type a triple decker and one type c triple decker, whereas **Dyad1** consists of two type c triple deckers. In addition, in **Dyad2** and **Dyad3** one europium is replaced by cerium, which provides for additional oxidation states in the information-storage molecule. For the preparation of **Dyad1–3**, we initially chose the hindered base DIEA as recommended in Pd-coupling reactions involving the *S*-acetylthiophenyl group.[33] However, we found that in all three cases upon use of DIEA, the formation of the triple-decker dyad proceeded very slowly and was accompanied by the formation of considerable amounts of oligomeric side-products as indicated by analytical SEC. The formation of significant amounts of higher molecular weight material is also observed in Pd-coupling reactions with porphyrins.[2,31] To overcome the problems of long reaction times, low yields, and the loss of starting material due to the formation of oligomers, we decided to employ TEA in place of DIEA in the following Pd-mediated coupling reactions. Coupling reactions involving TEA have proved successful for the (*S*-acetylthiomethyl)aryl group,[3,34] which is more stable than the *S*-acetylthiophenyl group, and is used as the linker in our case.

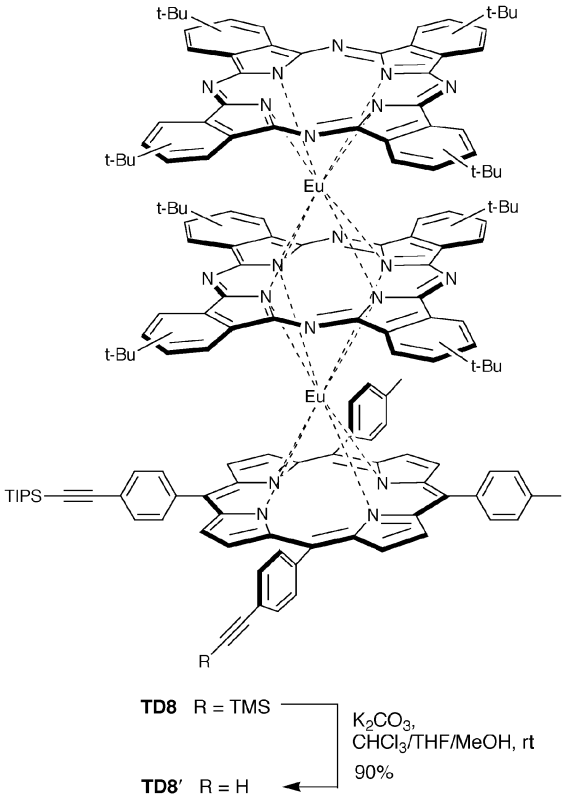

Scheme 4

Horizontal dyads with one linker (H1). An H1 dyad analogous to **Dyad3** was prepared to investigate the influence of the different architectures of triple-decker dyads on the electrochemical properties in solution as well as in SAMs. For this purpose, ethynylphenyl triple decker **AcS-TD11′** was treated with iodophenyl triple decker **TD9**, applying the reaction conditions described above with use of TEA instead of DIEA (Scheme 12). The reaction was monitored by analytical SEC and by LD-MS. The reaction proceeded faster than those employing DIEA and was stopped after 8.5 h. However, further catalyst had to be added twice. The desired **Dyad4** was obtained in 38% yield after chromatography on silica, SEC (THF), and again on silica. LD-MS (POPOP) showed the molecule ion peak at m/z = 4975.8. Note that **Dyad4** is isomeric to **Dyad3** with the *S*-acetylthiomethyl linker *cis* instead of *trans* to the inter-triple decker axis.

Horizontal dyads with two linkers (H2). In the H2 dyads, each triple decker bears one *S*-acetylthiomethyl linker for attachment to the gold surface. As stated above, this arrangement is anticipated to prevent rotation of the triple-decker moieties around the bridging ethyne group upon binding to a surface, but a mixture of *syn*/*anti* isomers will also be present. For purposes of comparing the H1 and H2 architectures, we prepared the H2 dyad analogous to **Dyad4**, substituted with a thiol-attachment unit at both triple deckers.

Applying the same reaction conditions as for the synthesis of **Dyad4**, iodophenyl triple decker **TD11** was coupled with ethynylphenyl triple decker **TD8′** (Scheme 13). Note that both **TD11** and **TD8′** each incorporate one *cis*-A_2BC porphyrin. After 5.5 h, analytical SEC indicated ~67% of product **TMS/TIPS-Dyad5**, and the reaction was stopped.[32] In contrast to the coupling reactions involving DIEA, almost no oligomeric species were present in the reaction mixture. The desired dyad was isolated in 59% yield after a two-column procedure. The TIPS and TMS groups of **TMS/TIPS-Dyad5** were both cleaved in one step by treatment with (n-Bu_4)NF in THF at room

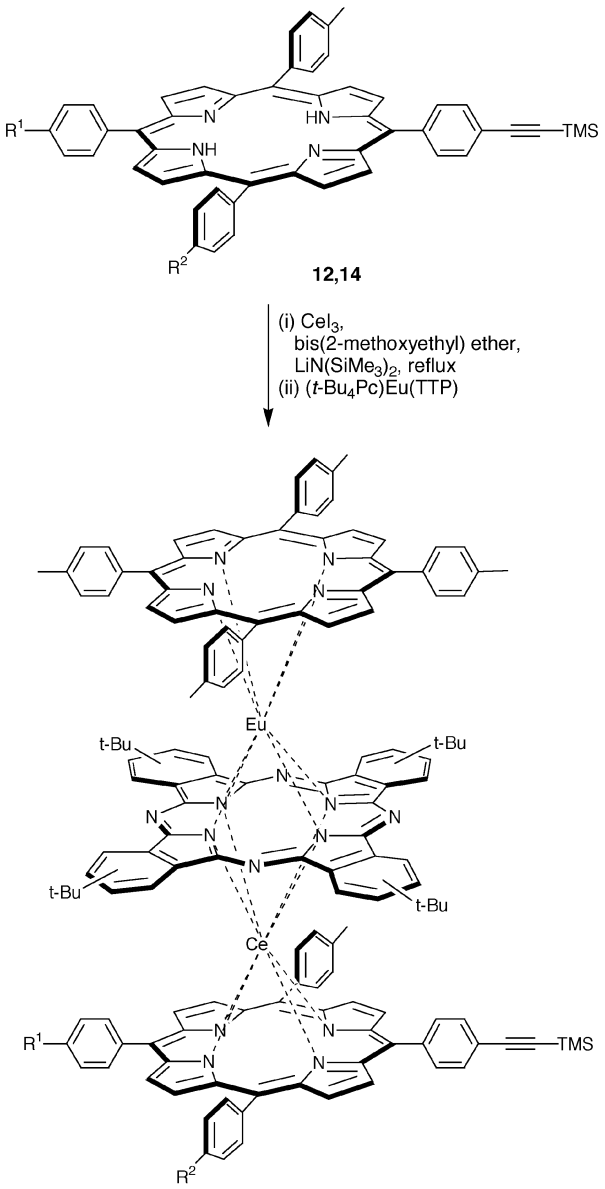

Porphyrin	R^1	R^2	Triple Decker	Yield
12	CH_3	I	**TD11**	54%
14	I	CH_3	**TD3**	46%

Scheme 5

temperature. LD-MS showed that deprotection was complete after 1 h, affording **Dyad5′** in 96% yield. The *S*-acetylthiomethyl-linker groups were then introduced by Sonogashira coupling [$Pd_2(dba)_3$, P(*o*-tol)$_3$, toluene–TEA (5 : 1), 35 °C] of **Dyad5′** with excess 1-(*S*-acetylthiomethyl)-4-iodobenzene (**17**),[2] affording the desired **Dyad5** in 42% yield. LD-MS showed the molecule ion peak at m/z = 5155.7 together with peaks at m/z = 5080.8 and 4980.6 owing to cleavage of the linker groups. **Dyad5** consists of a large number of isomers due to the four *syn*/*anti* architectures and the presence of the four patterns of *tert*-butyl groups on each phthalocyanine ligand. The four *syn*/*anti* architectures are expected to exhibit distinct spatial demands as shown in Fig. 4.

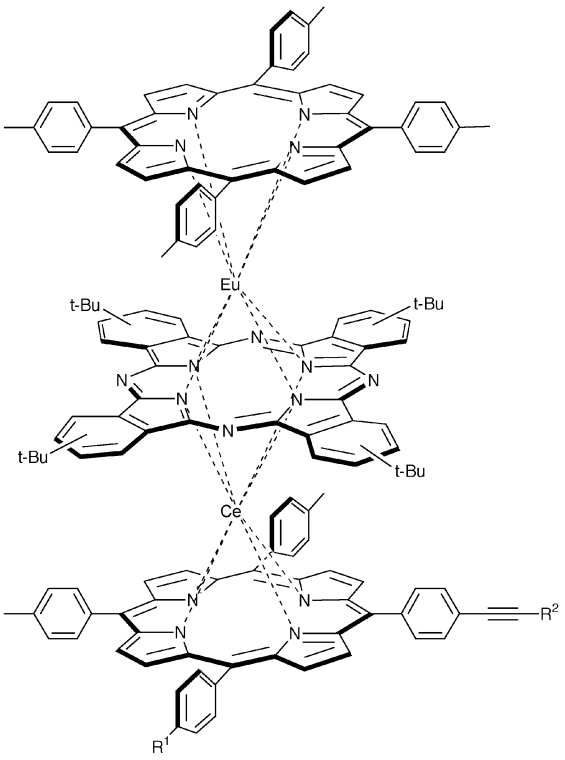

R^1	R^2	Triple Decker
I	TMS	**TD11**
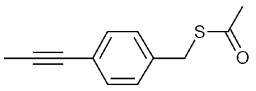	TMS	**AcS-TD11** (57%)
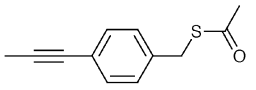	H	**AcS-TD11′** (66%)

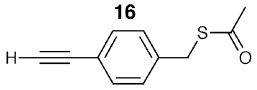

$Pd(PPh_3)_2Cl_2$, CuI
THF, TEA, 35 °C

$(n\text{-Bu})_4NF$, THF, 0 °C

Scheme 6

3 General characterization of triple-decker building blocks and dyads

The triple-decker building blocks and dyads were assessed for homogeneity by thin layer chromatography (TLC) and by analytical SEC. Characterization was generally performed by absorption spectroscopy, LD-MS, ^{1}H NMR spectroscopy, and fast-atom bombardment mass spectrometry (FAB-MS). Many of the triple deckers and all of the *S*-acetylthiomethyl-derivatized dyads were characterized electrochemically in solution, and all of the latter were also characterized electrochemically in SAMs.

Mass spectra. LD-MS has proved particularly effective for identifying the desired lanthanide porphyrin/phthalocyanine complexes. The triple-decker monomers each display the molecule ion peak together with characteristic fragmentation peaks upon analysis without a matrix. For the dyads, the best spectra were obtained employing POPOP as a matrix. In addition, a FAB-MS spectrum was obtained for each of **Dyad1–4**. Samples of **TMS/TIPS-Dyad5**, **Dyad5′**, and **Dyad5** did not ionize.

Absorption spectra. The UV–Vis spectra of the triple-decker monomers exhibit absorptions at 362–364 nm for type a (**AcS-TD3**, **AcS-TD3′**, **TD11**, **AcS-TD11**, **AcS-TD11′**) and at 345–348 nm for type c (**TD7**, **AcS-TD7**, **AcS-TD7′**, **TD8**, **TD8′**, **TD9**, **TD10**), which are attributed to the B-band of the phthalocyanine moieties. Absorptions in the region at 421–427 nm for type a and at 416–418 nm for type c are assigned to the porphyrin B-band. The remaining absorption in the visible region is attributed to the Q-bands of the macrocycles, in which the lower-energy Q-bands are contributed mainly by the phthalocyanine.[35] The data are in good agreement with those reported for similar heteroleptic triple-decker (phthalocyaninato)(porphyrinato)Eu(III)[6,9,36,37] and Ce(III) complexes.[38,39] Interestingly, the different substituents at the aryl groups of the porphyrins within two series (type a triple deckers **TD3**, **AcS-TD3**, **AcS-TD3′**, **TD11**, **AcS-TD11**, **AcS-TD11′**; type c triple deckers **TD8**, **TD8′**, **TD9**) do not induce a substantial shift of the absorption maxima, an observation noted by Ng for some Eu(III) triple-decker complexes.[9] In the case of type a triple deckers, the porphyrin B-band is broadened or split owing to the presence of two different porphyrins. Due to the decrease in ratio of porphyrin : phthalocyanine when going from type a (2 : 1) to type c (1 : 2); this band is the most intense in the spectra for type a, whereas the phthalocyanine B-band is dominant for type c.[9,36,38,39] Similar features are observed for the triple-decker dyads, and their absorption spectra are essentially the sum of the spectra of the corresponding monomers. The phthalocyanine B-band of **Dyad2–5** (comprised of type a and type c) is located at 350–353 nm (between that of type a and type c triple deckers). The porphyrin B-band is broadened or split and shows the highest intensity. In the

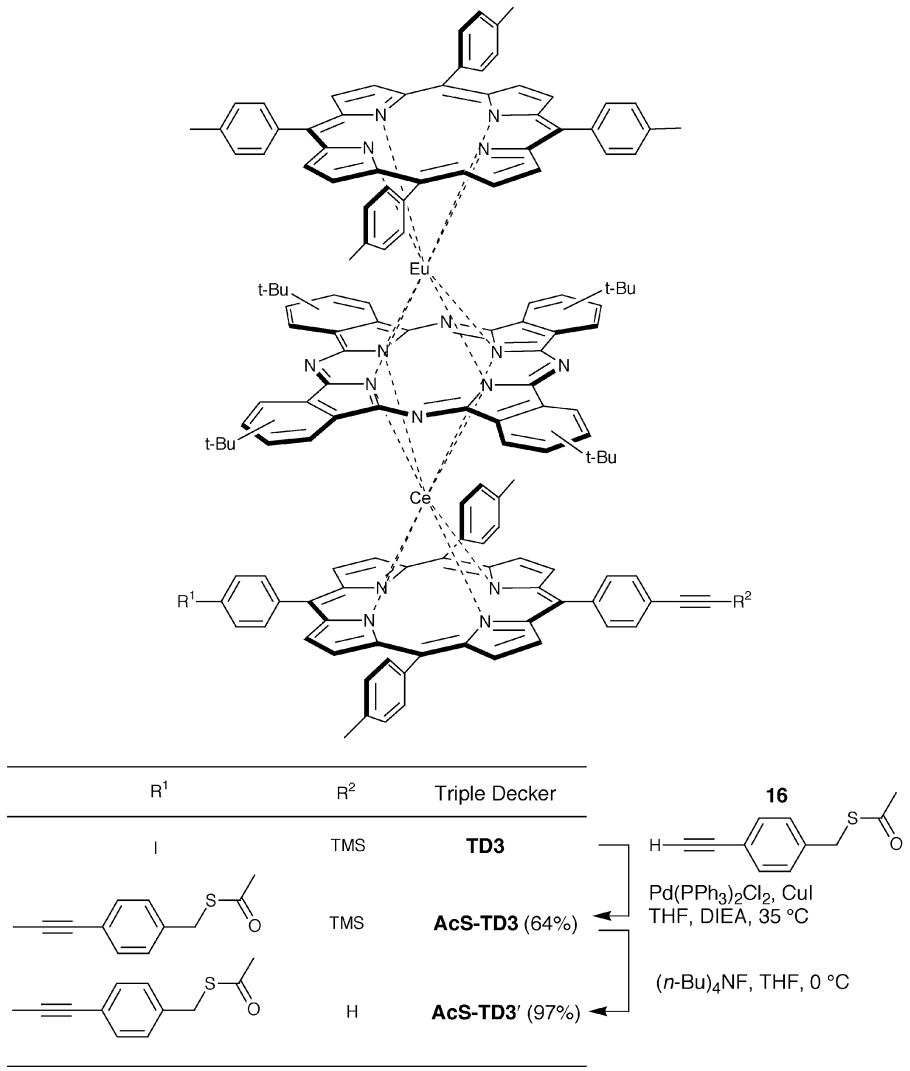

Scheme 7

case of the only type c/type c dyad (**Dyad1**), the phthalocyanine B-band is the most intense absorption band. Thus, a simple inspection of the UV/Vis spectra allows distinction between type a/type c and type c/type c triple-decker dyads.

^{1}H NMR spectra. Heteroleptic triple-decker complexes with paramagnetic metal centers such as Ce(III) and Eu(III) give ^{1}H NMR spectra wherein the signals are generally broad and spread over a wide region.[35] In addition, the presence of one or more tetra-*tert*-butylphthalocyanine ligand (comprised of four regioisomers) in each triple decker caused the ^{1}H NMR spectra of the triple-decker monomers and dyads to be very complex and difficult to interpret.[30] In particular, the aromatic protons result in broad (eventually overlapping) multiplet signals. Restricted rotation along the C(*meso*)–C(aryl) bonds in porphyrins of symmetrical type a and type c Eu(III) triple-decker complexes has been attributed as the source of 4 or 5 signals for the *meso*-phenyl protons.[9,36] The triple deckers of type c (**TD8**, **TD8′**, **TD9**, **TD10**) are comprised of two nonequivalent phthalocyanine rings (inner and outer in the sandwich complex) and a porphyrin bearing 3 or 4 non-equivalent *meso*-aryl rings, which further complicates the spectra. Nevertheless, by comparison with data for similar symmetrical triple deckers,[6,9,36,40] multiplets at δ = 13.6–12.6, 11.26–11.24, 11.0–8.6, 7.4–7.1, 6.8, and 5.4–5.0 ppm can be attributed to the α and β protons of the phthalocyanines and to the *meso*-phenyl protons of the porphyrin moiety. The *tert*-butyl groups on the phthalocyanine macrocycle together with the β-pyrrole protons of the porphyrin ligand give rise to a broad multiplet in the range of 3.6–2.5 ppm. Specific assignments can be made for some significant signals. A singlet at δ = 0.84 ppm in the spectrum of **TD8** is ascribed to the TMS group. This signal is absent in the spectrum of **TD8′**, showing complete deprotection. Instead, a singlet is observed at δ = 3.86 ppm due to the free ethyne group. The TIPS group in **TD8** or **TD8′** gives rise to a sharp peak at δ = 1.77 or 1.75 ppm, respectively.

Triple deckers of type a (**AcS-TD3**, **AcS-TD3′**, **TD11**, **AcS-TD11**, **AcS-TD11′**) contain two different porphyrins (TTP and a porphyrin bearing 3 or 4 nonequivalent phenyl rings). The signals are generally shifted to higher fields owing to the presence of one Ce instead of Eu in the triple-decker complex.[14,41] The TMS groups in **TD11**, **AcS-TD11**, and **AcS-TD3** result in a singlet between δ = −0.05 and −0.08 ppm. After deprotection, a singlet is found at δ = 2.56 ppm for the ethyne proton in **AcS-TD11′** or **AcS-TD3′**. The *S*-acetylthiomethyl linker groups in each of **AcS-TD3**, **AcS-TD3′**, **AcS-TD11**, and **AcS-TD11′** give rise to singlets at δ = 2.26–2.27 and 3.96–3.98 ppm.

The ^{1}H NMR spectra of the triple-decker dyads are even more complex owing to the superimposed (complex) spectra of the corresponding monomers. However, as in the case for the monomers, singlet signals at δ = 2.61 and 4.44 ppm for **Dyad1** and at δ = 2.31–2.32 and 4.01–4.06 ppm for **Dyad2–5** are attributable to the *S*-acetylthiomethyl linker(s) attached to one or both triple-decker moieties.

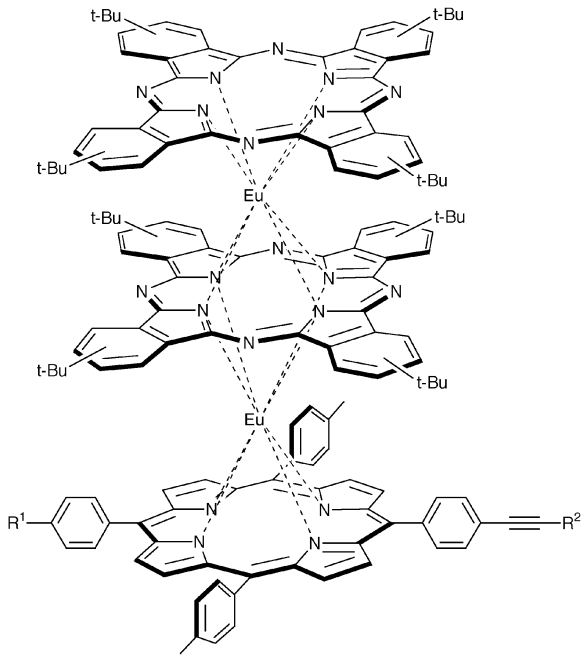

R^1	R^2	Triple Decker
I	TMS	**TD7**
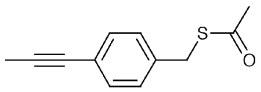	TMS	**AcS-TD7** (59%)
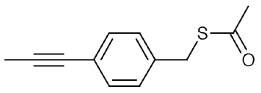	H	**AcS-TD7′** (89%)

16

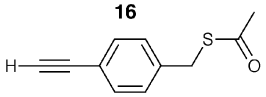

$Pd(PPh_3)_2Cl_2$, CuI
THF, DIEA, 35 °C

$(n\text{-Bu})_4NF$, THF, 0 °C

Scheme 8

TD10 + **AcS-TD7′**

$Pd_2(dba)_3$, P(*o*-tol)$_3$,
toluene, DIEA, 35 °C

25%

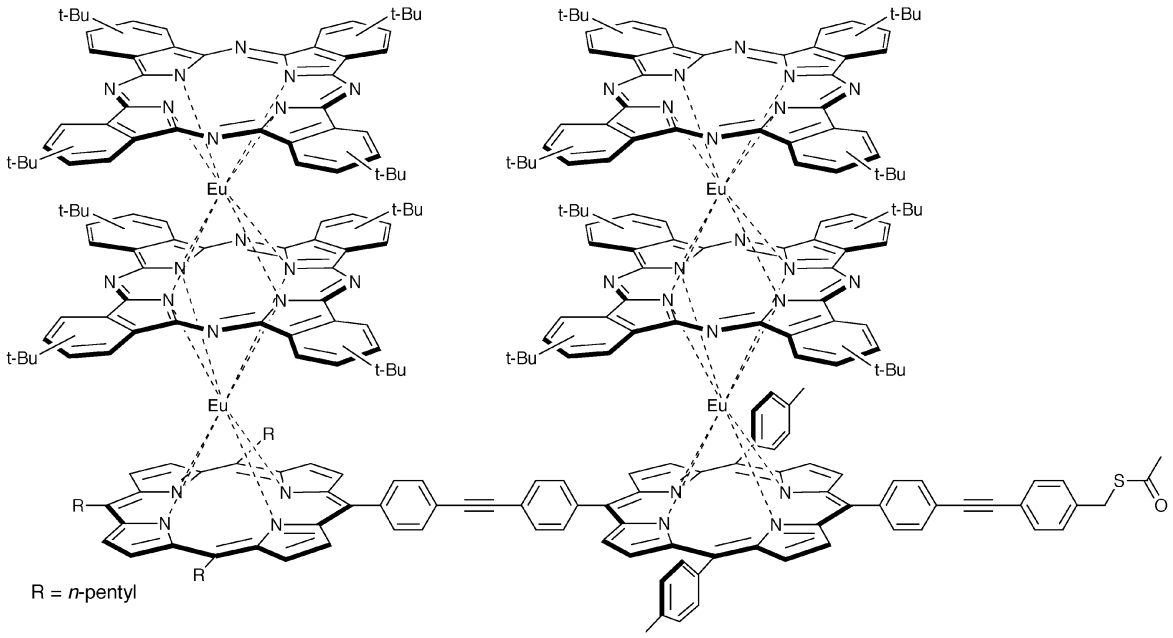

Dyad1

Scheme 9

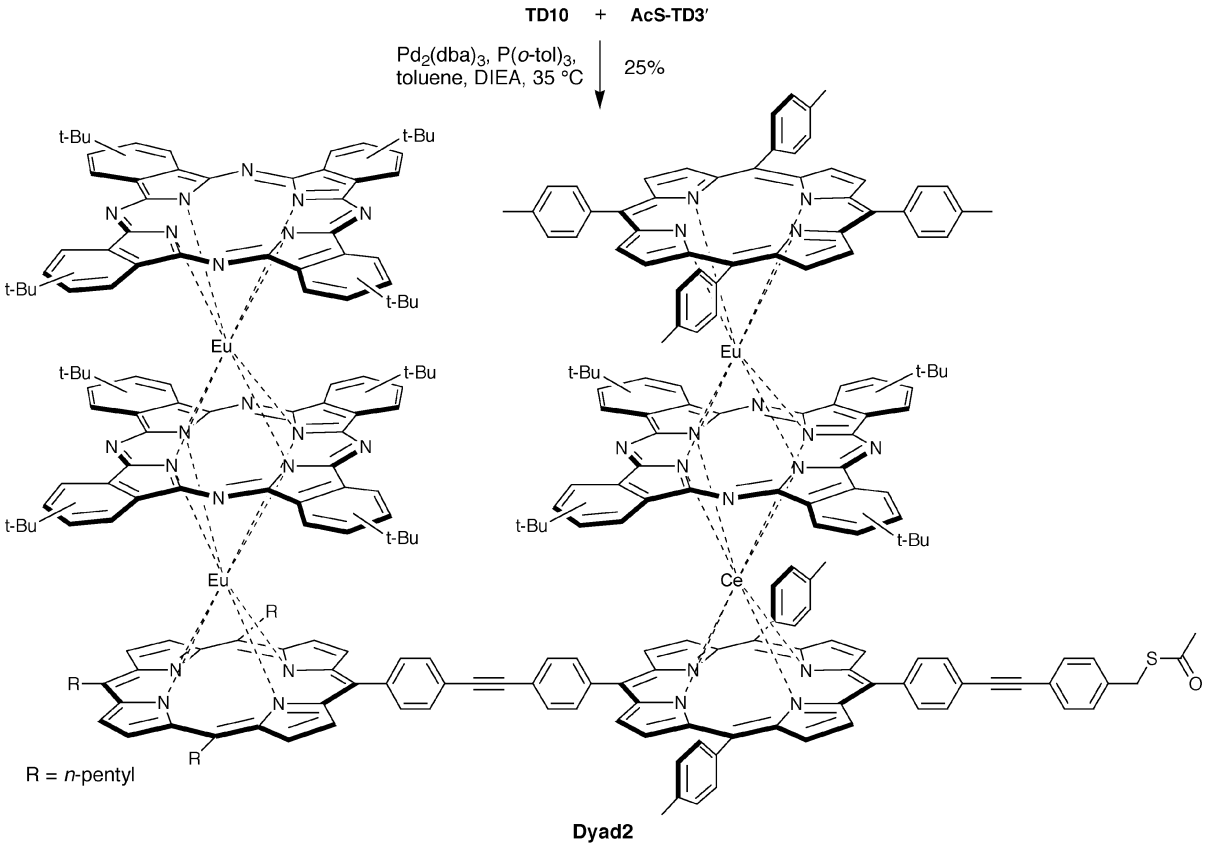

Dyad2

Scheme 10

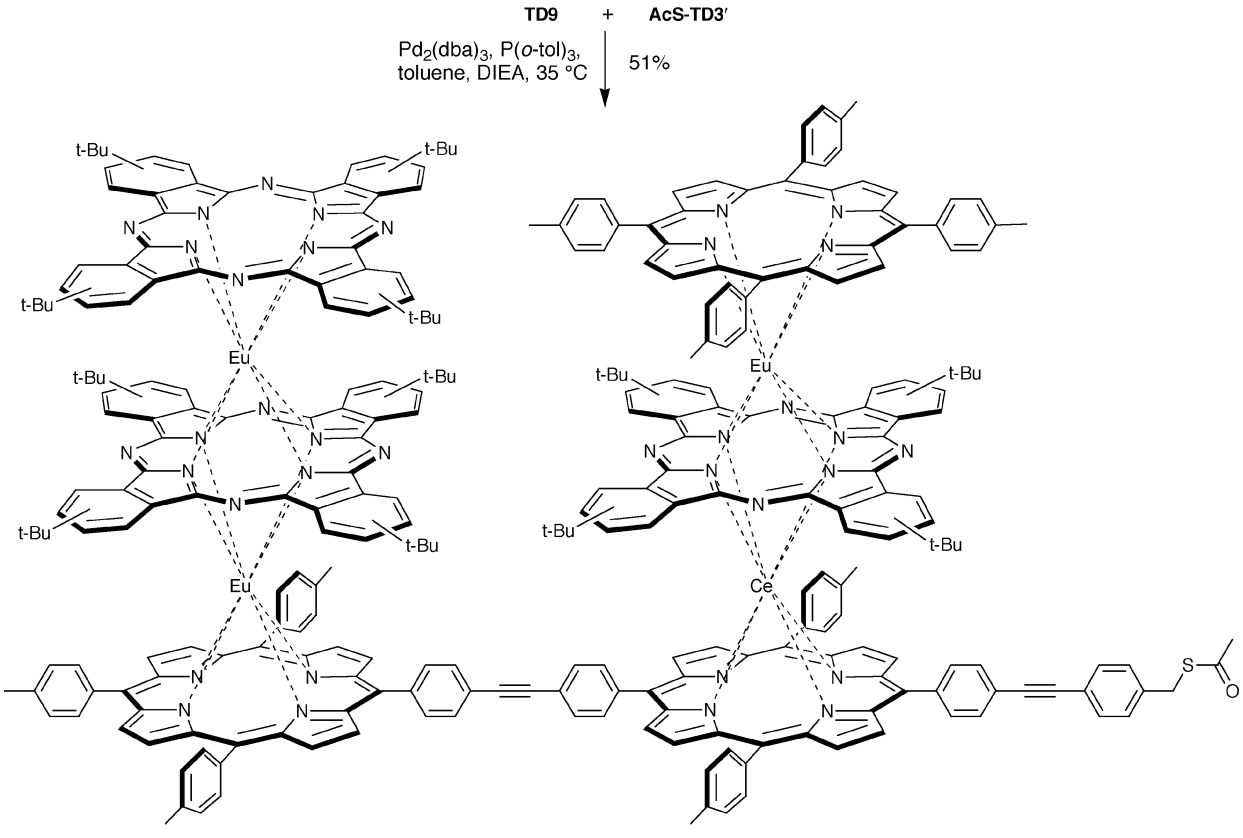

Dyad3

Scheme 11

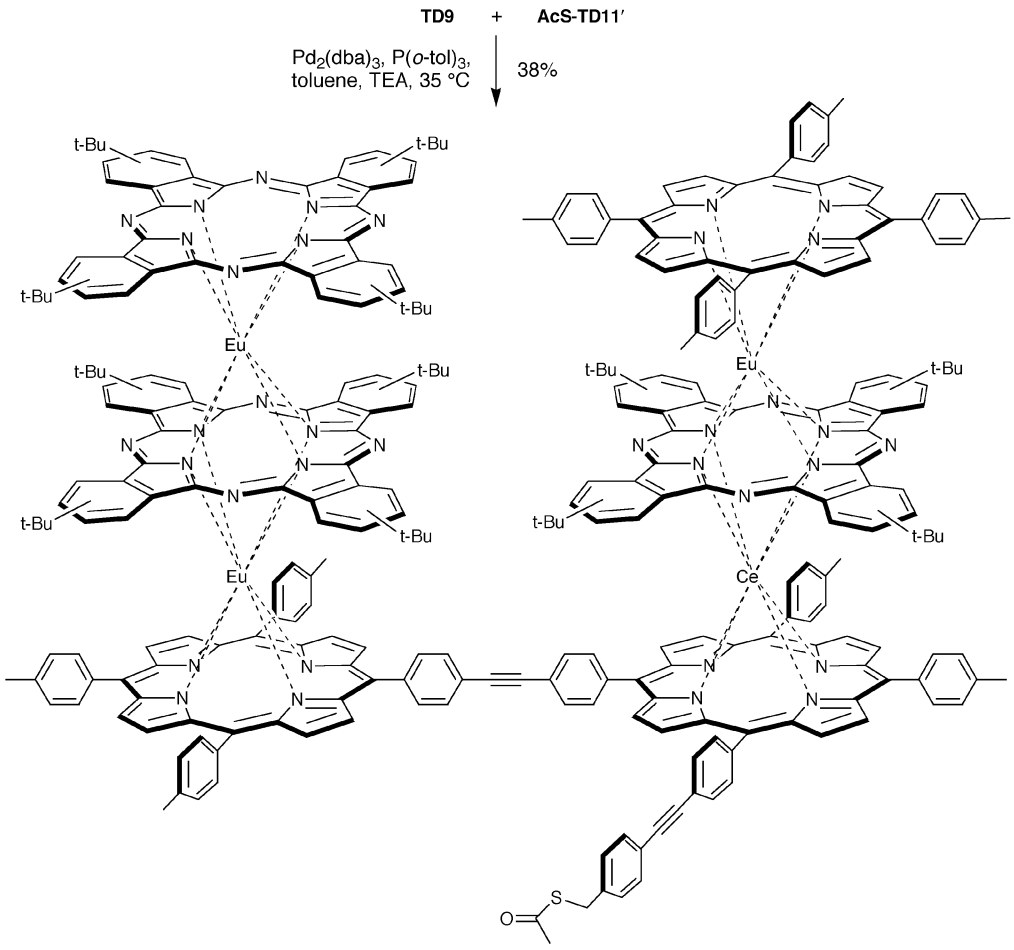

Scheme 12

4 Electrochemical characteristics of the dyads in solution and in SAMs

Solution. The solution electrochemical properties of **Dyad1–5** were examined and compared with those of the most structurally similar triple-decker benchmark complexes. These benchmarks are as follows: **Dyad1**, **TD4/TD6**; **Dyad2**, **TD3/TD6**; **Dyad3–5**, **TD3/TD4**. The square-wave voltammograms of **Dyad1–5** are shown in Fig. 5–9 (top panels). The potentials for all five dyads are summarized in Table 2. In the table, the potentials are listed in order of increasing value. Accordingly, each successive pair of values for a dyad corresponds to the lower potential for each of the two triple deckers in the dyad (*i.e.*, dyad ($E_{0/+1}$/$E_{+1/+2}$) corresponds to $TD^{\alpha}(E_{0/+1})$/$TD^{\beta}(E_{0/+1})$; dyad($E_{+2/+3}$/$E_{+3/+4}$) corresponds to $TD^{\alpha}(E_{+1/+2})$/$TD^{\beta}(E_{+1/+2})$, *etc.*, where TD^{α} and TD^{β} denote the two triple deckers in the dyad). Comparison of the data in Tables 1 and 2 shows that the solution redox potentials of the dyads are quite close to those of the benchmark triple deckers. In all cases, the potentials for the analogous states of the dyads and the benchmark triple deckers differ by 0.05 V or less. The largest differences in potential (albeit small) occur for **Dyad1** and **Dyad2** where one of the *meso*-pentyl substituents of the porphyrin in the benchmark triple decker is replaced by a diphenylethyne linker. The potential differences are negligible for the other dyads because the diphenylethyne linker and the (*S*-acetylthiomethyl)diarylethyne linker(s) have very similar electron-donating properties to that of the aryl group of the benchmark triple deckers.

SAMs. Representative fast-scan (100 V s^{-1}) voltammograms of the SAMs of **Dyad1–5** are compared with the solution data in Fig. 5–9 (bottom panels). The oxidation potentials for the SAMs of all five dyads are summarized in Table 2. In general, the voltammograms of the SAMs of all five dyads are of excellent quality and are far superior to those obtained for the mixed monolayers of triple-decker monomers that we previously examined.[7] These results indicate that the strategy of covalently linking the triple deckers is key to obtaining a viable multistate counter. In addition, all three architectures appear to be robust. Closer inspection of the data for the dyad SAMs reveals a number of other features. These features are discussed in more detail below.

(1) The quality of the voltammograms for the dyad SAMs appears to be dependent on the composition of constituent triple deckers. In particular, the V1 dyads **Dyad1** and **Dyad2**, both of which contain a *meso*-pentyl-substituted porphyrin in the upper triple decker, give superior voltammetry to **Dyad3**, which contains a *meso*-aryl-substituted porphyrin in this unit. This is evidenced by the fact that **Dyad3** appears to exhibit a subset of oxidation waves that are shifted to lower potential than the principal peaks (see Fig. 7, bottom panel). For example, additional waves are evident at $\sim$0.93 V and $\sim$0.02 V. These lower potential waves could correspond to a minority domain wherein the dyads are more poorly packed (hence the lower potential, *vide infra*) than the majority domain. The additional oxidation waves are absent in the SAMs of the horizontal **Dyad4** and **Dyad5** (although there is a hint of another wave at $\sim$0.82 V for the former dyad). Thus, it is possible that certain dyads are better suited for a horizontal architecture than a vertical one (and *vice versa*). Additional studies on dyads of like composition in horizontal *vs.* vertical architectures will be required to fully elucidate this issue.

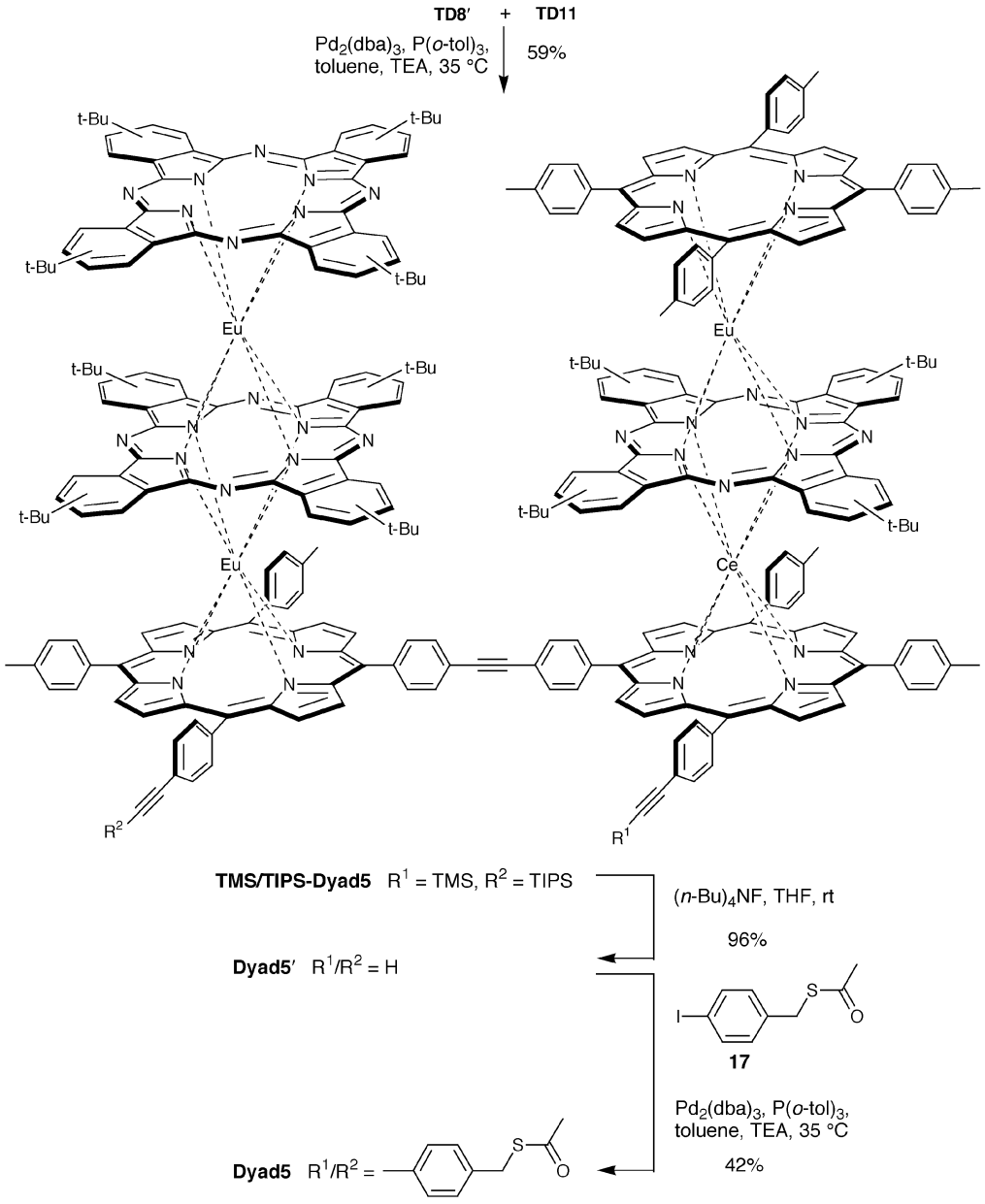

Scheme 13

(2) For each of **Dyad1–5**, the oxidation potential for a particular wave in the SAM is generally more positive than the corresponding wave in solution by 0.05–0.20 V. This behavior is consistent with our previous studies of porphyrin SAMs.[2–7] However, **Dyad5** does not follow this trend. For this dyad, the oxidation potentials of the SAM are generally lower than those observed for the solution. We have no clear explanation for this phenomenon. The positive shift in redox potentials observed upon SAM formation has generally been attributed to poorer access of counterions to the redox center due to packing of the molecules on the surface.[42] If so, the absence of a positive potential-shift would suggest relatively poor packing. In this regard, the area per molecule occupied by **Dyad5** is much larger than that of any of the other dyads (*vide infra*). This could be due to the fact that **Dyad5** is in an H2 architecture, which renders the molecule more rigid and perhaps compromises packing on the surface.

(3) For each of the V1 dyads **Dyad1–3**, the potentials of the lower *vs.* upper triple deckers do not appear to be differentially shifted upon SAM formation. This is evident from the fact that the splittings between the pairs of *E*-values that correspond to oxidation of each triple decker in the dyad are qualitatively similar in solution and in the SAMs. For example, in the case of **Dyad2**, the splitting between $E_{0/+1}$ and $E_{+1/+2}$ is 0.22 V in solution and 0.18 V in the SAM; the splitting between $E_{+2/+3}$ and $E_{+3/+4}$ is $\sim$0.17 V in solution and 0.15 V in the SAM (see Table 2). Likewise for **Dyad1**, the waves for $E_{0/+1}$ and $E_{+1/+2}$ are overlapped in both the solution and the SAM. This behavior shows that for the design of an optimum multistate counter, it is not necessary to consider differential surface effects (at least for the redox potential) on the upper and lower members of vertical dyads.

(4) The surface area measurements indicate that dyads in the vertical architecture generally occupy less surface area than those in the horizontal architectures. In particular, the average area for the three V1 structures (**Dyad1–3**) is $\sim$760 Å^2 molecule^{-1}, whereas the areas for the H1 (**Dyad4**) and H2 (**Dyad5**) structures are $\sim$1640 Å^2 molecule^{-1} and 2700 Å^2 molecule^{-1}, respectively. All of these areas are relatively large compared with those that might be expected for a closest-packed structure. Based on the molecular dimensions, closest packing of the V1 dyads would yield areas of $\sim$300 Å^2 molecule^{-1}; closest packing of the H1 or H2 dyads would yield areas of $\sim$700 Å^2 molecule^{-1} (assuming (1) no torsional

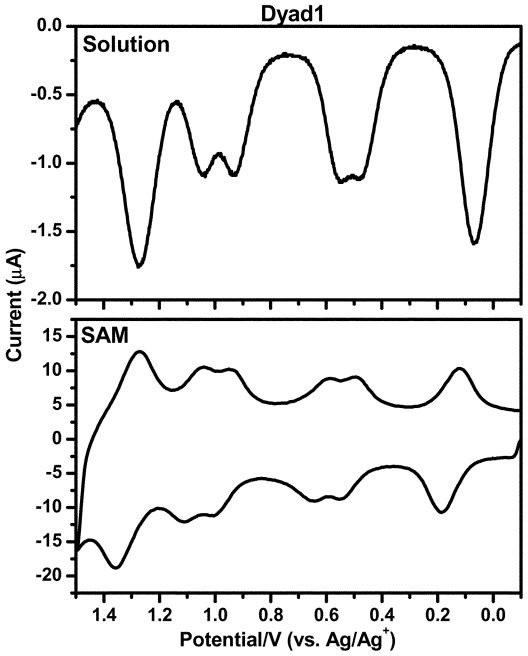

Fig. 5 Voltammetry of **Dyad1** in solution (top panel) and in a SAM (bottom panel). The solvent was CH_2Cl_2 containing 0.1 M (solution) or 1.0 M (SAM) Bu_4NPF_6; the scan rate was 0.1 V s^{-1} (solution) or 100 V s^{-1} (SAM).

rotation for the V1 and H1 structures about the –C≡C– bond of the linker and (2) a perpendicular orientation of the macrocycle planes with respect to the surface). The larger areas for the V1 and H1 architectures could be due to torsional rotation. The very large area for the H2 structure could result from the added rigidity of the molecule upon binding to the surface (as noted above); the presence of *syn versus anti* isomers of this dyad could also contribute. Regardless, the fact that the vertical architecture generally results in more dense packing of the dyads is an important design consideration for a viable multistate counter. On nanoplatforms, more dense packing would

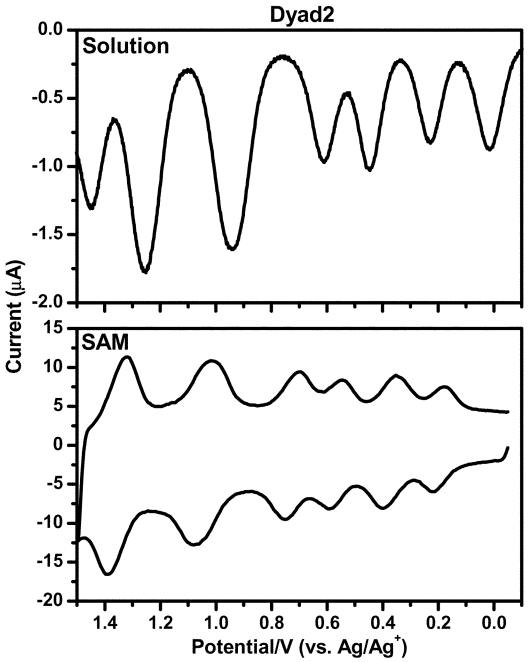

Fig. 6 Voltammetry of **Dyad2** in solution (top panel) and in a SAM (bottom panel). The solvent was CH_2Cl_2 containing 0.1 M (solution) or 1.0 M (SAM) Bu_4NPF_6; the scan rate was 0.1 V s^{-1} (solution) or 100 V s^{-1} (SAM).

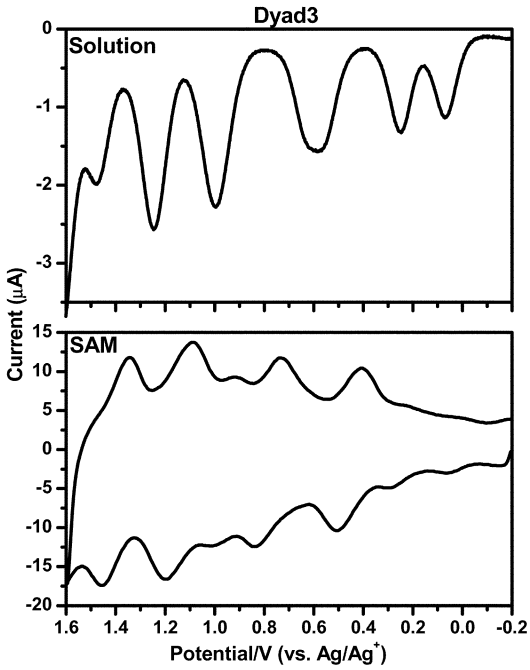

Fig. 7 Voltammetry of **Dyad3** in solution (top panel) and in a SAM (bottom panel). The solvent was CH_2Cl_2 containing 0.1 M (solution) or 1.0 M (SAM) Bu_4NPF_6; the scan rate was 0.1 V s^{-1} (solution) or 100 V s^{-1} (SAM).

afford more facile detection of electrical signals from the molecules in the SAM.

Conclusions

We have described the design of covalently linked dyads of lanthanide porphyrinic triple-decker complexes with interleaving cationic oxidation potentials that could be used in a molecular multistate counter. Five dyads were prepared by Pd-catalyzed coupling (Sonogashira reaction) of appropriately functionalized triple-decker building blocks (type a or type c).

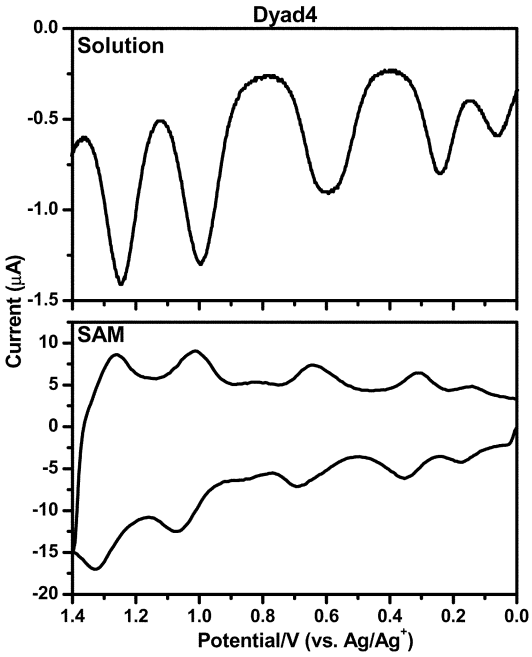

Fig. 8 Voltammetry of **Dyad4** in solution (top panel) and in a SAM (bottom panel). The solvent was CH_2Cl_2 containing 0.1 M (solution) or 1.0 M (SAM) Bu_4NPF_6; the scan rate was 0.1 V s^{-1} (solution) or 100 V s^{-1} (SAM).

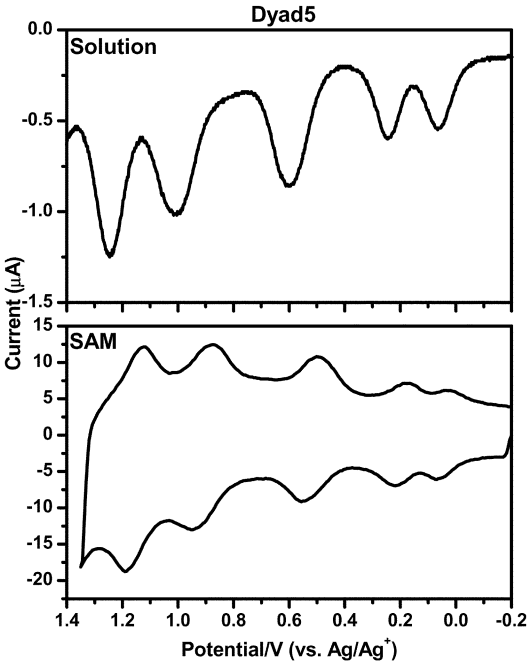

Fig. 9 Voltammetry of **Dyad5** in solution (top panel) and in a SAM (bottom panel). The solvent was CH_2Cl_2 containing 0.1 M (solution) or 1.0 M (SAM) Bu_4NPF_6; the scan rate was 0.1 V s^{-1} (solution) or 100 V s^{-1} (SAM).

The porphyrins in the triple deckers and the triple deckers themselves were prepared by rational synthetic methods. Three of the five dyads were constituted for a vertical architecture (V1), bearing one *S*-acetylthiomethyl group for attachment to an electroactive gold surface, whereas the other two dyads were designed for a horizontal arrangement with one (H1) or two (H2) *S*-acetylthiomethyl linkers.

The electrochemical characteristics of the five thiol-derivatized dyads were investigated both in solution and in SAMs. The dyad SAMs generally yield robust, reversible voltammograms with features comparable to those observed in solution (albeit with some shifts in potential). This behavior can be contrasted with that observed for mixtures of non-covalently linked triple-decker complexes. These complexes exhibit poorly resolved redox waves indicative of a highly heterogeneous, poorly packed SAM. The covalent linkage essentially overcomes this problem. The high quality voltammetric characteristics of the dyad SAMs indicate that these constructs are excellent candidates for multistate counters that could be used for storage of information at the molecular level.

Experimental

General

^1H NMR spectra were collected in $CDCl_3$ (300 MHz) unless noted otherwise. Absorption spectra (HP 8451A, Cary 3) were collected in toluene. Porphyrins and triple-decker sandwich complexes were analyzed by LD-MS (Bruker Proflex II) and FAB-MS (JEOL HX 110HF), either in high (HR) or low resolution (LR). High-resolution mass spectrometry was carried out at greater than unit resolution. LD-MS analysis was done without a matrix or with the matrix POPOP.[43]

All operations involving organometallic compounds and Pd-catalyzed couplings were carried out under an inert atmosphere of argon using standard Schlenk techniques. $Eu(acac)_3 \cdot nH_2O$ was obtained from Alfa Aesar. Unless otherwise indicated, all other reagents were obtained from Aldrich Chemical Company, and all solvents were obtained from Fisher Scientific.

Non-commercial compounds

The following compounds were prepared as described in the literature: dipyrromethanes **1**,[25] **2**,[24] and **3**;[25] *S*-2-pyridyl (4-methyl)thiobenzoate (**4**);[27] acid chlorides **6** and **7**;[24] diacyl dipyrromethane **10**;[28] porphyrins **14**[24] and **15**;[6] double-decker complexes[16] (TTP)Eu(*t*-Bu_4Pc) and (*t*-$Bu_4Pc)_2$Eu;[14,29] and thiol-protected linkers **16** and **17**.[2] Triple deckers **TD1**,[7] **TD2**,[14] **TD3**,[14] **TD4**,[7] **TD5**,[14] and **TD6**[7] have been prepared previously.

Chromatography

Adsorption column chromatography was performed using flash silica (Baker, 60–200 mesh). Preparative-scale SEC was performed using BioRad Bio-beads SX-1 in THF and eluted with gravity flow.[44] Analytical-scale SEC was performed with a Hewlett-Packard 1090 HPLC using a 1000 Å column (5 μL, styrene–divinylbenzene copolymer) with THF as eluent (0.8 mL min^{-1}).[44] Preparative-scale TLC was performed on silica gel plates (Merck, 60 F_{254}s, layer thickness 0.5 mm).

1-(4-Methylbenzoyl)-5-(4-methylphenyl)dipyrromethane (5)

Following a standard procedure,[27] a solution of EtMgBr (43 mL, 43 mmol, 1.0 M in THF) was slowly added *via* syringe to a stirred solution of dipyrromethane **1** (4.06 g, 17.2 mmol) in THF (17 mL) under Ar. The mixture was stirred at room temperature for 10 min and then cooled to −78 °C. *S*-2-Pyridyl (4-methyl)thiobenzoate (**4**) (3.94 g, 17.2 mmol) was then added, and the mixture was maintained at −78 °C for 30 min. The cooling bath was removed, and the mixture was maintained at

Table 2 Potentials for the oxidation of the dyads in solution[a] and in SAMs[b]

Potential/V[c]								
Dyad	$E_{0/+1}$	$E_{+1/+2}$	$E_{+2/+3}$	$E_{+3/+4}$	$E_{+4/+5}$	$E_{+5/+6}$	$E_{+6/+7}$	$E_{+7/+8}$
Solution								
Dyad1	~0.07	~0.07	0.48	0.55	0.94	1.05	~1.28	~1.28
Dyad2	0.01	0.23	0.44	0.61	~0.94	~0.94	~1.25	~1.25
Dyad3	0.07	0.24	~0.58	~0.58	~0.99	~0.99	~1.24	~1.24
Dyad4	0.06	0.24	~0.58	~0.58	~0.99	~0.99	~1.24	~1.24
Dyad5	0.07	0.25	~0.60	~0.60	~1.01	~1.01	~1.25	~1.25
SAM								
Dyad1	~0.15	~0.15	0.52	0.61	0.98	1.08	~1.31	~1.31
Dyad2	0.20	0.38	0.57	0.72	~1.05	~1.05	~1.35	~1.35
Dyad3	0.26	0.46	~0.78	~0.78	~1.14	~1.14	~1.40	~1.40
Dyad4	0.16	0.35	~0.67	~0.67	~1.04	~1.04	~1.29	~1.29
Dyad5	0.05	0.20	~0.53	~0.53	~0.91	~0.91	~1.16	~1.16

[a]Obtained in CH_2Cl_2 containing 0.1 M Bu_4NPF_6. *E*-values *vs.* Ag/Ag^+; $FeCp_2/FeCp_2^+$ = 0.19 V; scan rate = 0.1 V s^{-1}. Values are ±0.03 V. [b]Obtained in CH_2Cl_2 containing 1.0 M Bu_4NPF_6. *E*-values *vs.* Ag/Ag^+; $FeCp_2/FeCp_2^+$ = 0.19 V; scan rate = 100 V s^{-1}. [c]*E*-values are listed as approximate because the oxidation waves for the two triple deckers in the dyad overlap.

room temperature for 30 min. The reaction was quenched with saturated aqueous NH_4Cl. The mixture was poured into ethyl acetate. The organic layer was washed with water, dried (Na_2SO_4), and concentrated, affording a dark foam. Purification by flash column chromatography [silica, neat CH_2Cl_2 to CH_2Cl_2–ethyl acetate (100 : 3)] afforded a golden amorphous solid (4.56 g, 75%): mp 77–81 °C; ^{1}H NMR δ 2.48 (s, 3H), 2.58 (s, 3H), 5.67 (s, 1H), 6.14 (m, 1H), 6.24 (m, 1H), 6.30 (m, 1H), 6.83 (m, 1H), 6.96 (m, 1H), 7.20–7.30 (m, 4H), 7.41 (d, J = 7.8 Hz, 2H), 7.89 (d, J = 7.8 Hz, 2H), 8.35 (br s, 1H), 9.88 (br s, 1H); ^{13}C NMR δ 18.7, 21.3, 21.8, 44.0, 107.8, 108.7, 110.5, 110.6, 117.8, 120.5, 128.4, 129.2, 129.3, 129.7, 130.8, 131.4, 135.9, 137.2, 137.9, 141.7, 142.5, 184.5; FAB-MS obsd (HR) 354.1754, calcd exact mass 354.1732 ($C_{24}H_{22}N_2O$); Anal. Calcd for $C_{24}H_{22}N_2O$: C, 81.33; H, 6.26; N, 7.90. Found: C, 80.69; H, 6.34; N, 7.73%.

1-{4-[2-(Triisopropylsilyl)ethynyl]benzoyl}-9-(4-methylbenzoyl)-5-(4-methylphenyl)dipyrromethane (8)

Following a standard procedure,[24] to a stirred solution of monoacyl dipyrromethane **5** (1.45 g, 4.09 mmol) in dry toluene (16 mL) at room temperature was slowly added EtMgBr (8 mL, 8 mmol, 1.0 M in THF) under Ar, and the mixture was stirred for 5 min. To the resulting mixture was added **6** (1.31 g, 4.08 mmol). After 10 min, the same process was repeated once [8 mL, 8 mmol, 1.0 M in THF of EtMgBr, and 1.31 g, 4.08 mmol of **6**]. After stirring for 10 min, the mixture was treated with additional EtMgBr (4 mL, 4 mmol, 1.0 M in THF) followed by **6** (0.64 g, 2.0 mmol). After stirring the contents for 20 min, saturated aqueous NH_4Cl (50 mL) and ethyl acetate (120 mL) were added. The organic layer was separated, dried (Na_2SO_4), and concentrated. Purification by column chromatography [silica, neat CH_2Cl_2, then CH_2Cl_2–ethyl acetate (98 : 2, then 98 : 3, then 90 : 10)] followed by slow precipitation from propan-2-ol afforded a pink amorphous solid (1.69 g, 65%): mp 142–143 °C; ^{1}H NMR δ 1.13 (s, 21H), 2.38 (s, 3H), 2.40 (s, 3H), 5.61 (s, 1H), 5.95–5.99 (m, 2H), 6.51–6.56 (m, 2H), 7.20 (d, J = 8.1 Hz, 4H), 7.41 (d, J = 7.8 Hz, 2H), 7.49 (d, J = 8.1 Hz, 2H), 7.68 (d, J = 8.4 Hz, 2H), 7.71 (d, J = 8.4 Hz, 2H), 11.28 (s, 1H), 11.32 (s, 1H); ^{13}C NMR δ 11.5, 18.9, 21.4, 21.8, 44.8, 93.9, 106.6, 111.3, 111.6, 120.7, 121.1, 127.0, 128.9, 129.6, 129.8, 129.9, 131.1, 131.3, 131.8, 135.7, 137.4, 137.8, 140.9, 141.8, 142.4, 183.6, 184.5; FAB-MS obsd (HR) 638.3262, calcd exact mass 638.3329 ($C_{42}H_{46}N_2O_2Si$); Anal. Calcd for $C_{42}H_{46}N_2O_2Si$: C, 78.95; H, 7.26; N, 4.38. Found: C, 78.74; H, 7.29; N, 4.26%.

1-(4-Iodobenzoyl)-9-(4-methylbenzoyl)-5-(4-methylphenyl)dipyrromethane (9)

Following the procedure described for **8**,[24] monoacyl dipyrromethane **5** (1.77 g, 4.99 mmol) in dry toluene (20 mL) was treated with EtMgBr (25 mL, 25 mmol, 1.0 M in THF) and 4-iodobenzoyl chloride (**7**) (3.33 g, 12.5 mmol) under Ar at room temperature. Purification by column chromatography [silica, CH_2Cl_2–ethyl acetate (98 : 2, then 97 : 3)] followed by slow precipitation from propan-2-ol afforded a pink amorphous solid (1.98 g, 68%): mp 139–141 °C; ^{1}H NMR δ 2.38 (s, 3H), 2.40 (s, 3H), 5.61 (s, 1H), 5.95–6.00 (m, 2H), 6.52–6.60 (m, 2H), 7.20 (d, J = 8.1 Hz, 4H), 7.39 (d, J = 8.1 Hz, 2H), 7.48 (d, J = 8.4 Hz, 2H), 7.68 (d, J = 8.1 Hz, 2H), 7.76 (d, J = 8.4 Hz, 2H), 11.22 (s, 1H), 11.25 (s, 1H); ^{13}C NMR δ 14.3, 21.4, 21.8, 22.7, 31.8, 44.9, 99.2, 111.3, 111.6, 120.7, 121.1, 128.2, 128.88, 128.91, 129.8, 130.0, 130.8, 131.26, 131.30, 135.7, 137.36, 137.42, 137.44, 137.8, 141.0, 142.1, 142.4, 183.5, 184.5; FAB-MS obsd (HR) 584.0944, calcd exact mass 584.0961 ($C_{31}H_{25}IN_2O_2$); Anal. Calcd for $C_{31}H_{25}IN_2O_2$: C, 63.71; H, 4.31; N, 4.79. Found: C, 65.24; H, 4.57; N, 4.68%.

5-{4-[2-(Triisopropylsilyl)ethynyl]phenyl}-15,20-bis(4-methylphenyl)-10-{4-[2-(trimethylsilyl)ethynyl]phenyl}porphyrin (11)

Following a standard procedure,[24] a solution of **8** (420 mg, 0.65 mmol) in a mixture of dry THF–methanol (10 : 1, 29 mL) under a stream of Ar at room temperature was treated with $NaBH_4$ (497 mg, 13.1 mmol, 20 mol equiv) in small portions (~0.1 g every 2 min) with rapid stirring. The progress of the reaction was monitored by TLC [alumina, CH_2Cl_2–ethyl acetate (3 : 2) and silica, CH_2Cl_2–ethyl acetate (5 : 1)]. After the reaction was complete (about 45 min), the reaction mixture was poured into a stirred mixture of saturated aqueous NH_4Cl (40 mL) and CH_2Cl_2 (80 mL). The organic phase was washed with water, dried (Na_2SO_4), and placed in a 500 mL round-bottomed flask. Removal of the solvent under reduced pressure yielded the dicarbinol as a solid (~0.65 mmol). A sample of dipyrromethane **2** (208 mg, 0.65 mmol) was added followed by acetonitrile (265 mL). TFA (613 μL, 7.96 mmol) was then added, and the reaction was monitored by UV/Vis spectroscopy. After 3 min, DDQ (438 mg, 1.93 mmol) was added, and the mixture was stirred at room temperature for 1 h. Then triethylamine (1.11 mL, 7.96 mmol) was added, and the entire reaction mixture was filtered through a pad of alumina (eluted with CH_2Cl_2) until the eluent was no longer dark. After removal of the solvent, column chromatography [silica, CH_2Cl_2–hexanes (1 : 1)] afforded a purple solid (121 mg, 20%): ^{1}H NMR δ −2.80 (s, 2H), 0.38 (s, 9H), 1.26 (s, 21H), 2.71 (s, 6H), 7.56 (d, J = 7.8 Hz, 4H), 7.85–7.89 (m, 4H), 8.09 (d, J = 7.2 Hz, 4H), 8.15 (d, J = 7.5 Hz, 4H), 8.78–8.88 (m, 8H); LD-MS obsd 921.3 [M^+], 878.0, 848.5, 837.9, 821.4, 807.4, 792.3; FAB-MS obsd (HR) 918.4527, calcd exact mass 918.4513 ($C_{62}H_{62}N_4Si_2$); λ_{abs} 423, 517, 552, 594, 649 nm.

5-(4-Iodophenyl)-15,20-bis(4-methylphenyl)-10-{4-[2-(trimethylsilyl)ethynyl]phenyl}porphyrin (12)

Analogous to the preparation of **11**,[24] a sample of diacyl dipyrromethane **9** (1.35 g, 2.31 mmol) was reduced with $NaBH_4$ (1.75 g, 46.3 mmol) in dry THF–methanol (10 : 1, 110 mL), affording the dicarbinol as a foam-like solid (~2.31 mmol). The resulting dicarbinol was reacted with dipyrromethane **2** (736 mg, 2.31 mmol). Column chromatography [silica, CH_2Cl_2–hexanes (1 : 1)] afforded a purple solid (420 mg, 21%): ^{1}H NMR δ −2.81 (s, 2H), 0.38 (s, 9H), 2.71 (s, 6H), 7.56 (d, J = 7.8 Hz, 4H), 7.87 (d, J = 8.1 Hz, 2H), 7.94 (d, J = 8.1 Hz, 2H), 8.09 (d, J = 6.9 Hz, 6H), 8.16 (d, J = 8.1 Hz, 2H), 8.79–8.89 (m, 8H); LD-MS obsd 864.1 [M^+], 782.1, 767.2, 739.1 [M^+ − I]; FAB-MS obsd (HR) 864.2137, calcd exact mass 864.2145 ($C_{51}H_{41}IN_4Si$); λ_{abs} 422, 516, 552, 593, 649 nm.

5-(4-Iodophenyl)-10,15,20-tris(4-methylphenyl)porphyrin (13)

Analogous to the preparation of **11**,[24] a sample of diacyl dipyrromethane **10** (220 mg, 0.47 mmol) was reduced with $NaBH_4$ (351 mg, 9.31 mmol) in dry THF–methanol (10 : 1, 11 mL), affording the dicarbinol as an orange oil (~0.47 mmol). The resulting dicarbinol was reacted with dipyrromethane **3** (258 mg, 0.47 mmol). Column chromatography [silica, hexanes–CH_2Cl_2 (3 : 2)] afforded a purple solid (77 mg, 21%): ^{1}H NMR δ −2.80 (s, 2H), 2.71 (s, 9H), 7.56 (d, J = 7.5 Hz, 6H), 7.95 (d, J = 8.1 Hz, 2H), 8.09 (d, J = 8.1 Hz, 8H), 8.80–8.97 (m, 8H); LD-MS obsd 782.8 [M^+], 656.5 [M^+–I]; FAB-MS obsd (HR) 783.2005, calcd exact mass 783.1985 ($C_{47}H_{35}IN_4$); λ_{abs} 376, 421, 486, 516, 551, 593, 649 nm.

TD7

Following a standard procedure,[13,14] a mixture of $Eu(acac)_3 \cdot nH_2O$ (319 mg) and porphyrin **14** (87 mg, 0.10 mmol) in 1,2,4-trichlorobenzene (11 mL) was stirred at 220 °C under a slow

stream of Ar for 8 h. After cooling to room temperature, a sample of $(t\text{-}Bu_4Pc)_2Eu$ (163 mg, 0.10 mmol) was added, and the mixture was refluxed under Ar for a further 14 h. After removal of the solvent, purification by column chromatography (silica, $CHCl_3$), then SEC (THF) and finally by a silica column ($CHCl_3$) afforded a dark-green solid (195 mg, 74%): ^{1}H NMR δ 0.84 (s, 9H), 2.03 (s, 6H), 2.2–4.1 (m, 80H), 4.99–5.22 (m, 4H), 6.81 (m, 2H), 7.13 (m, 1H), 7.35 (m, 1H), 8.4–11.0 (m, 24H), 11.28 (m, 4H), 12.4–13.8 (m, 12H); LD-MS obsd 2640.3 [M^+], 2514.1 [$M^+ - I$]; FAB-MS obsd (HR) 2640.84; calcd exact mass 2640.84 ($C_{147}H_{135}Eu_2IN_{20}Si$); λ_{abs} 346, 418, 526, 622, 728 nm.

TD8

Following a standard procedure,[13,14] a mixture of $Eu(acac)_3 \cdot nH_2O$ (136 mg) and porphyrin **11** (42.0 mg, 45.7 μmol) in 1,2,4-trichlorobenzene (5 mL) was stirred at 220 °C under a slow stream of Ar for 6 h to form the corresponding europium porphyrin half-sandwich complex. After cooling to room temperature, a sample of $(t\text{-}Bu_4Pc)_2Eu$ (74.8 mg, 46.0 μmol) was added, and the mixture was again refluxed under Ar for a further 5 h. After removal of the solvent, purification by column chromatography [silica, CH_2Cl_2] afforded a dark-green solid, which was further purified by SEC (THF) and finally a silica column (CH_2Cl_2) (97 mg, 79%): ^{1}H NMR δ 0.84 (s, 9H), 1.38 (s, 3H), 1.77 (s, 21H), 1.98 (s, 3H), 2.5–3.6 (m, 80 H), 5.12–5.36 (m, 4H), 6.81 (m, 2H), 7.22 (m, 2H), 8.6–11.0 (m, 16H), 11.26 (m, 4H), 12.6–13.6 (m, 12H); LD-MS obsd 2693.2 [M^+], 2678.5, 2663.9; FAB-MS obsd (LR) 2695.26, calcd exact mass 2695.08 ($C_{158}H_{156}Eu_2N_{20}Si_2$); λ_{abs} 347, 419, 527, 621, 729 nm.

TD8′

A sample of **TD8** (54.5 mg, 20.2 μmol) in a mixture of $CHCl_3$–THF–methanol (1 : 5 : 2, 8 mL) was treated with powdered K_2CO_3 (71.8 mg, 0.52 mmol) and stirred under Ar at room temperature for 5 h. The progress of the reaction was monitored by LD-MS. Then the reaction mixture was filtered. The filtrate was washed with 10% aqueous $NaHCO_3$ (100 mL) and water (150 mL). The organic layer was dried (Na_2SO_4), concentrated and chromatographed (silica, CH_2Cl_2), affording a dark-green solid (47.8 mg, 90%): ^{1}H NMR δ 1.36 (s, 3H), 1.75 (s, 21H), 1.90 (s, 3H), 2.5–3.6 (m, 80H), 3.86 (br s, 1H), 5.10–5.28 (m, 4H), 6.79 (br s, 2H), 7.16 (br s, 2H), 8.6–11.0 (m, 16H), 11.23 (m, 4H), 12.4–13.6 (m, 12H); LD-MS obsd 2627.7 [M^+], 2613.1, 2518.7, 2461.2; FAB-MS obsd (LR) 2623.20, calcd exact mass 2623.04 ($C_{155}H_{148}Eu_2N_{20}Si$); λ_{abs} 347, 418, 527, 621, 729 nm.

TD9

Following a standard procedure,[13,14] a mixture of $Eu(acac)_3 \cdot nH_2O$ (117 mg) and porphyrin **13** (28.7 mg, 36.7 μmol) in 1,2,4-trichlorobenzene (4 mL) was stirred at 220 °C under a slow stream of Ar for 6 h. After cooling to room temperature, a sample of $(t\text{-}Bu_4Pc)_2Eu$ (60.1 mg, 36.7 μmol) was added, and the mixture was again refluxed under Ar for a further 5 h. After removal of the solvent, purification by column chromatography [silica, $CHCl_3$ (containing 0, 1 and 5% ethyl acetate, respectively)] afforded a dark-green solid, which was further purified by SEC (THF) and finally a silica column ($CHCl_3$) (58 mg, 62%): ^{1}H NMR δ 1.35 (s, 3H), 1.94 (s, 6H), 2.5–3.6 (m, 80H), 5.00–5.17 (m, 4H), 6.80 (br s, 3H), 7.34 (m, 1H), 8.6–9.3 (m, 4H), 9.40 (br s, 3H), 9.7–11.0 (m, 9H), 11.25 (m, 4H), 12.6–13.5 (m, 12H); LD-MS obsd 2556.1 [M^+], 2429.5 [$M^+ - I$]; FAB-MS obsd (HR) 2558.75, calcd exact mass 2558.82 ($C_{143}H_{129}Eu_2IN_{20}$); λ_{abs} 346, 417, 526, 620, 727 nm.

TD10

Following a standard procedure,[13,14] a mixture of $Eu(acac)_3 \cdot nH_2O$ (221 mg) and porphyrin **15** (50.0 mg, 69.2 μmol) in 1,2,4-trichlorobenzene (7.6 mL) was stirred at 220 °C under a slow stream of Ar for 5 h. After cooling to room temperature, a sample of $(t\text{-}Bu_4Pc)_2Eu$ (113 mg, 69.2 μmol) was added, and the mixture was refluxed under Ar for a further 14 h. After removal of the solvent, the residue was chromatographed (silica, $CHCl_3$). Further purification by SEC (THF), a silica column ($CHCl_3$), and finally again by SEC (THF) afforded 43 mg (25%) of a dark-green solid. A ^{1}H NMR spectrum was recorded, but the complexity due to the mixture of regioisomers prevented a complete interpretation. LD-MS obsd 2496.7 [M^+], 2482.0, 2439.9, 2371.0 [$M^+ - I$]; FAB-MS obsd (LR) 2498.71, calcd exact mass 2498.91 ($C_{137}H_{141}Eu_2IN_{20}$); λ_{abs} 345, 416, 530, 581, 627, 733 nm.

TD11

The following is a refined version of the standard procedure[14] designed to minimize exposure of the reaction mixture to moisture and air. A Schlenk flask was equipped with a reflux condenser and all essential inlets and outlets at the beginning of the procedure. A solution of $CeI[N(SiMe_3)_2]_2$ was prepared *in situ* by reaction of CeI_3 (75.0 mg, 0.144 mmol) and $LiN(SiMe_3)_2$ (288 μL, 0.288 mmol, 1.0 M in THF) in bis(2-methoxyethyl) ether (1.5 mL). This flask was not opened. A deaerated solution of porphyrin **12** (25.0 mg, 28.9 μmol) in bis(2-methoxyethyl) ether (1 mL) was added by syringe. The mixture was refluxed for 1 h, affording the metalated porphyrin as determined by UV/Vis. Then the double-decker complex (TTP)Eu(t-Bu_4Pc) (45.2 mg, 28.9 μmol) was added. The mixture was refluxed for 6 h. After cooling to room temperature, chromatography [silica, toluene–hexanes (1 : 1), then CH_2Cl_2] gave three bands (green). The first and second bands were combined and concentrated, affording a solid, which was further purified by SEC (THF), affording a brownish-green solid (40 mg, 54%): A ^{1}H NMR spectrum was recorded, but the complexity due to the mixture of regioisomers prevented a complete interpretation. LD-MS obsd 2557.5 [M^+], 2542.9, 2459.8, 2431.7 [$M^+ - I$]; FAB-MS obsd (LR) 2559.86, calcd exact mass 2559.72 ($C_{147}H_{123}CeEuIN_{16}Si$); λ_{abs} 363, 421, 425, 492, 560, 609 nm.

AcS-TD3

A 25 mL Schlenk flask containing samples of **TD3** (26.1 mg, 10.2 μmol), 1-[4-(*S*-acetylthiomethyl)phenyl]acetylene (**16**) (39.2 mg, 205 μmol), $Pd(PPh_3)_2Cl_2$ (2.4 mg, 3.4 μmol), and CuI (0.3 mg, 1.6 μmol) was evacuated and purged with Ar three times. Then deaerated THF (2.5 mL) and deaerated DIEA (0.4 mL) were added, and the reaction mixture was stirred under Ar at 35 °C for 7 h. After removal of the solvent, the residue was redissolved in toluene and chromatographed on silica (toluene). Further purification by SEC (THF) and finally a silica column (toluene) afforded an olive-green solid (17 mg, 64%). A ^{1}H NMR spectrum was recorded, but the complexity due to the mixture of regioisomers prevented a complete interpretation. LD-MS obsd 2631.5 [M^+], 2553.0 [$M^+ - SAc$]; FAB-MS obsd (HR) 2621.82, calcd exact mass 2621.85 ($C_{158}H_{132}CeEuN_{16}OSSi$); λ_{abs} 363, 421, 427, 492, 560, 609 nm.

AcS-TD7

A 50 mL Schlenk flask containing samples of **TD7** (174 mg, 65.9 μmol), **16** (126 mg, 659 μmol), $Pd(PPh_3)_2Cl_2$ (14.1 mg, 19.8 μmol), and CuI (1.9 mg, 9.9 μmol) was evacuated and purged with Ar three times. THF (25 mL) and DIEA (3.4 mL) were added, and the reaction mixture was stirred under Ar at 35 °C for 6 h. The progress of the reaction was monitored by

LD-MS. After removal of the solvent, the residue was purified by column chromatography [silica, $CHCl_3$ (containing 0, then 2, then 5% ethyl acetate)] to afford a dark-green solid, which was further purified by SEC (toluene) and finally preparative TLC [silica, toluene–diethyl ether (20 : 1)] (105 mg, 59%): ^{1}H NMR δ 0.80 (s, 9H), 1.84 (s, 6H), 2.0–3.6 (m, 80H), 2.62 (s, 3H), 4.45 (s, 2H), 5.08–5.21 (m, 4H), 6.78 (br s, 2H), 7.05–7.16 (m, 2H), 7.71 (d, J = 8.1 Hz, 2H), 8.08 (d, J = 7.5 Hz, 2H), 8.5–11.0 (m, 16H), 11.22 (m, 4H), 12.5–13.7 (m, 12H); LD-MS obsd 2707.0 [M^+], 2635.4 [M^+ − SAc]; FAB-MS obsd (LR) 2702.98, calcd exact mass 2702.97 ($C_{158}H_{144}Eu_2N_{20}OSSi$); λ_{abs} 346, 419, 527, 621, 728 nm.

AcS-TD11

A 25 mL Schlenk flask containing samples of **TD11** (15.0 mg, 5.86 μmol), **16** (38.1 mg, 200 μmol), $Pd(PPh_3)_2Cl_2$ (1.4 mg, 2.0 μmol), and CuI (0.2 mg, 1.1 μmol) was evacuated and purged with Ar three times. Then deaerated THF (1.5 mL) and deaerated TEA (0.3 mL) were added, and the reaction mixture was stirred under Ar at 35 °C for 2 h. After removal of the solvent, the residue was redissolved in CH_2Cl_2–hexanes (1 : 2) and chromatographed on silica [CH_2Cl_2–hexanes (1 : 2)], affording an olive-green solid (8.8 mg, 57%). A ^{1}H NMR spectrum was recorded, but the complexity due to the mixture of regioisomers prevented a complete interpretation. LD-MS obsd 2622.4 [M^+], 2546.0 [M^+ − SAc]; FAB-MS obsd (HR) 2621.82, calcd exact mass 2621.85 ($C_{158}H_{132}CeEuN_{16}OSSi$); λ_{abs} 363, 421, 426, 492, 560, 609, 676 nm.

AcS-TD3′

To a stirred solution of **AcS-TD3** (17 mg, 6.5 μmol) in dry THF (2 mL) at 0 °C was added (n-Bu)$_4$NF (7.1 μL, 1.0 M in THF). After stirring for 5 min at 0 °C, the reaction was quenched by addition of water (1 mL). The mixture was extracted with CH_2Cl_2. The organic layer was washed with water, dried (Na_2SO_4), concentrated, and purified by preparative TLC (silica, toluene), affording an olive-green solid (16 mg, 97%). A ^{1}H NMR spectrum was recorded, but the complexity due to the mixture of regioisomers prevented a complete interpretation. LD-MS obsd 2548.9 [M^+], 2473.6 [M^+ − SAc]; FAB-MS obsd (HR) 2549.82, calcd exact mass 2549.81 ($C_{155}H_{124}CeEuN_{16}OS$); λ_{abs} 363, 421, 427, 492, 560, 609 nm.

AcS-TD7′

To a stirred solution of **AcS-TD7** (90 mg, 33.3 μmol) in THF (5 mL) at 0 °C was added (n-Bu)$_4$NF (37 μL, 1.0 M in THF). After stirring for 5 min, the reaction was quenched by addition of water (3 mL), and the solution was extracted with $CHCl_3$, washed with water, and dried (Na_2SO_4). After removal of the solvent, purification by preparative TLC [silica, toluene–diethyl ether (30 : 1)] afforded a dark-green solid (78 mg, 89%): ^{1}H NMR δ 1.88 (s, 6H), 2.0–3.6 (m, 80H), 2.63 (s, 3H), 3.85 (s, 1H), 4.46 (s, 2H), 5.09–5.21 (m, 4H), 6.79 (br s, 2H), 7.16 (br s, 2H), 7.71 (d, J = 7.2 Hz, 2H), 8.09 (d, J = 7.5 Hz, 2H), 8.5–11.0 (m, 16H), 11.25 (m, 4H), 12.5–13.7 (m, 12H); LD-MS obsd 2630.8 [M^+], 2555.2 [M^+ − SAc], 1618.1 [(t-Bu$_4$Pc)$_2$Eu$^+$]; FAB-MS obsd (LR) 2631.21, calcd exact mass 2630.94 ($C_{155}H_{136}Eu_2N_{20}OS$); λ_{abs} 346, 419, 526, 620, 728 nm.

AcS-TD11′

To a stirred solution of **AcS-TD11** (8.0 mg, 3.0 μmol) in dry THF (1 mL) at 0 °C was added (n-Bu)$_4$NF (3.5 μL, 1.0 M in THF). After stirring for 6 min at 0 °C, the reaction was quenched by addition of water (1 mL). The mixture was extracted with CH_2Cl_2. The organic layer was washed with water, dried (Na_2SO_4), concentrated, and purified by preparative TLC (silica, toluene), affording an olive-green solid (5.1 mg, 66%). A ^{1}H NMR spectrum was recorded, but the complexity due to the mixture of regioisomers prevented a complete interpretation. LD-MS obsd 2549.5 [M^+], 2475.1 [M^+ − SAc]; FAB-MS obsd (HR) 2549.77, calcd exact mass 2549.81 ($C_{155}H_{124}CeEuN_{16}OS$); λ_{abs} 363, 421, 492, 560, 609, 676 nm.

Dyad1

A 25 mL Schlenk flask containing samples of **TD10** (10.0 mg, 4.00 μmol), **AcS-TD7′** (10.5 mg, 4.12 μmol), $Pd_2(dba)_3$ (0.61 mg, 0.67 μmol), and P(o-tol)$_3$ (1.63 mg, 5.36 μmol) was evacuated and purged with Ar three times. Then deaerated toluene (3.5 mL) and deaerated DIEA (0.7 mL) were added, and the reaction mixture was stirred under Ar at 35 °C. The progress of the reaction was monitored by analytical SEC. Because the reaction had stopped, further catalyst [$Pd_2(dba)_3$, 0.61 mg (0.67 μmol); P(o-tol)$_3$, 1.22 mg (4.02 μmol)] was added after 22 h and again after 31 h. After a total reaction time of 48 h, the solvent was removed. The residue was redissolved in toluene–diethyl ether (100 : 1) and loaded onto a silica column packed with the same solvent. Three bands were collected (first band: blue; second band: green). The desired product was collected in a third band (green), employing toluene–diethyl ether (20 : 1) as the eluent. Further purification by SEC (THF) gave five bands, from which the third band (green) contained the product. Impurities collected from the SEC column were finally removed by a silica column [toluene–diethyl ether (100 : 1, then 50 : 1)], affording a dark-green solid (5.0 mg, 25%). A ^{1}H NMR spectrum was recorded, but the complexity due to the mixture of regioisomers prevented a complete interpretation. LD-MS obsd (POPOP) 5001.2 [M^+], 4985.5, 4972.5, 4957.4, 4938.5, 4924.4 [M^+ − SAc]; FAB-MS obsd (LR) 5002.01, calcd exact mass 5001.93 ($C_{292}H_{276}Eu_4N_{40}OS$); λ_{abs} 350, 421, 427, 493, 530, 625 nm.

Dyad2

A 25 mL Schlenk flask containing samples of **TD10** (10.0 mg, 3.91 μmol), **AcS-TD3′** (10.2 mg, 4.00 μmol), $Pd_2(dba)_3$ (0.55 mg, 0.60 μmol), and P(o-tol)$_3$ (1.34 mg, 4.40 μmol) was evacuated and purged with Ar three times. Then deaerated toluene (3.5 mL) and deaerated DIEA (0.7 mL) were added, and the reaction mixture was stirred under Ar at 35 °C. The progress of the reaction was monitored by analytical SEC. Because the reaction had stopped, further catalyst [$Pd_2(dba)_3$ 0.55 mg (0.60 μmol) and P(o-tol)$_3$ 1.01 mg (3.32 μmol)] was added after 7 h and again after 18 h. After a total reaction time of 24 h, the solvent was removed. The residue was redissolved in toluene–diethyl ether (100 : 1) and loaded onto a silica column packed with the same solvent. The desired product was collected in the second band (green), employing toluene–diethyl ether (50 : 1) as the eluent. Further purification by SEC (THF) gave three bands, from which the second band (green) contained the product. Impurities collected from the SEC column were finally removed by a silica column [toluene–diethyl ether (50 : 1)], affording a dark-green solid (5.0 mg, 25%). A ^{1}H NMR spectrum was recorded, but the complexity due to the mixture of regioisomers prevented a complete interpretation. LD-MS obsd (POPOP) 4922.1 [M^+], 4876.2, 4848.2 [M^+ − SAc]; FAB-MS obsd (LR) 4921.77, calcd exact mass 4920.81 ($C_{292}H_{264}CeEu_3N_{36}OS$); λ_{abs} 352, 420, 493, 523, 616, 676, 726 nm.

Dyad3

A 25 mL Schlenk flask containing samples of **TD9** (6.0 mg, 2.4 μmol), **AcS-TD3′** (6.0 mg, 2.4 μmol), $Pd_2(dba)_3$ (0.34 mg, 0.37 μmol), and P(o-tol)$_3$ (0.84, 2.79 μmol) was evacuated and

purged with Ar three times. Then deaerated toluene (2 mL) and deaerated DIEA (0.4 mL) were added, and the reaction mixture was stirred under Ar at 35 °C. The progress of the reaction was monitored by analytical SEC. Because the reaction had stopped after 20 h, the same amount of catalyst was added again, and the mixture was stirred for a further 4 h. After removal of the solvent, the residue was redissolved in toluene and loaded onto a silica column packed with the same solvent. Elution with toluene gave two bands (first band: blue; second band: olive-green, containing starting triple decker). The desired product was collected in a third band, employing toluene–ethyl acetate (20 : 1) as the eluent. Further purification by SEC (THF) gave four bands. The first two bands (green) contained higher molecular weight material. The third band (green) contained the product and a fourth band contained triple-decker starting material. Impurities collected from the SEC column were finally removed by a silica column [toluene, then toluene–diethyl ether (50 : 1)], affording a green solid (6.0 mg, 51%). A ^{1}H NMR spectrum was recorded, but the complexity due to the mixture of regioisomers prevented a complete interpretation. LD-MS obsd (POPOP) 4979.4 [M^+], 4965.1, 4902.4 [M^+ − SAc]; FAB-MS obsd (LR) 4982.13, calcd exact mass 4980.72 ($C_{298}H_{252}CeEu_3N_{36}OS$); λ_{abs} 346, 420, 528, 625, 730 nm.

Dyad4

A 25 mL Schlenk flask containing samples of **TD9** (5.0 mg, 2.0 μmol), **AcS-TD11′** (4.0 mg, 1.6 μmol), $Pd_2(dba)_3$ (0.42 mg, 0.46 μmol), and P(*o*-tol)$_3$ (1.17 mg, 3.84 μmol) was evacuated and purged with Ar three times. Then deaerated toluene (1.0 mL) and deaerated TEA (250 μL) were added, and the reaction mixture was stirred at 35 °C. The progress of the reaction was monitored by analytical SEC and by LD-MS. Further batches of $Pd_2(dba)_3$ (0.42 mg, 0.46 μmol) and P(*o*-tol)$_3$ (1.17 mg, 3.84 μmol) were added after 2 h and again after 6 h. After a total reaction time of 8 h 30 min, the solvent was removed. The residue was dissolved in CH_2Cl_2 and loaded onto a silica column packed with the same solvent. Elution with CH_2Cl_2 gave two bands. The desired product was collected in the second band. Further purification by SEC (THF) and finally a silica column (CH_2Cl_2) afforded the desired product (3.0 mg, 38%). A ^{1}H NMR spectrum was recorded, but the complexity due to the mixture of regioisomers prevented a complete interpretation. LD-MS obsd (POPOP) 4975.8 [M^+], 4085.8 [M^+ − (*t*-Bu$_4$Pc)Eu]; FAB-MS obsd 4981.76 (LR), calcd exact mass 4980.72 ($C_{298}H_{252}CeEu_3N_{36}OS$); λ_{abs} 352, 420, 427, 493, 523, 615, 727 nm.

TMS/TIPS-Dyad5

A 25 mL Schlenk flask containing samples of **TD11** (12.1 mg, 4.73 μmol), **TD8′** (12.2 mg, 4.65 μmol), $Pd_2(dba)_3$ (1.0 mg, 1.1 μmol), and P(*o*-tol)$_3$ (2.8 mg, 9.2 μmol) was evacuated and purged with Ar three times. Then deaerated toluene (2.5 mL) and deaerated TEA (0.6 mL) were added, and the reaction mixture was stirred at 35 °C. The progress of the reaction was monitored by analytical SEC and by LD-MS. Further batches of $Pd_2(dba)_3$ (1.0 mg, 1.1 μmol) and P(*o*-tol)$_3$ (2.8 mg, 9.2 μmol) were added after 2 h and again after 3 h 40 min. After a total reaction time of 5 h 30 min, the solvent was removed. The residue was dissolved in toluene and loaded onto a silica column packed with the same solvent. Elution with toluene gave two bands. The desired product was collected in the second band. Further purification by SEC (THF) gave the desired product (14 mg, 59%). A ^{1}H NMR spectrum was recorded, but the complexity due to the mixture of regioisomers prevented a complete interpretation. LD-MS obsd (POPOP) 5050.5 [M^+], 4165.3 [M^+ − (*t*-Bu$_4$Pc)Eu]; calcd exact mass 5054.85 ($C_{302}H_{270}CeEu_3N_{36}Si_2$); λ_{abs} 353, 421, 492, 616, 729 nm.

Dyad5′

To a solution of **TMS/TIPS-Dyad5** (12.0 mg, 2.37 μmol) in THF (1 mL) at room temperature was added (*n*-Bu)$_4$NF (5.7 μL, 1.0 M in THF). After stirring for 1 h, the reaction was quenched by addition of water, and the mixture was extracted with CH_2Cl_2, washed with water, and dried (Na_2SO_4). After removal of the solvent, purification by column chromatography (silica, toluene) afforded a dark-green solid (11 mg, 96%). A ^{1}H NMR spectrum was recorded, but the complexity due to the mixture of regioisomers prevented a complete interpretation. LD-MS obsd (POPOP) 4825.8 [M^+], calcd exact mass 4826.67 ($C_{290}H_{242}CeEu_3N_{36}$); λ_{abs} 353, 421, 493, 616, 729 nm.

Dyad5

A 25 mL Schlenk flask containing samples of **Dyad5′** (11.0 mg, 2.28 μmol), 1-(*S*-acetylthiomethyl)-4-iodobenzene (**17**) (13.3 mg, 45.5 μmol), $Pd_2(dba)_3$ (1.0 mg, 1.1 μmol), and P(*o*-tol)$_3$ (2.8 mg, 9.2 μmol) was evacuated and purged with Ar three times. Then deaerated toluene (3 mL) and deaerated TEA (0.6 mL) were added, and the reaction mixture was stirred at 35 °C. The progress of the reaction was monitored by analytical SEC and by LD-MS. Further batches of $Pd_2(dba)_3$ (1.0 mg, 1.1 μmol) and P(*o*-tol)$_3$ (2.8 mg, 9.2 μmol) were added after 1 h 30 min and again after 4 h. After a total reaction time of 6 h, the solvent was removed. Purification by preparative TLC [silica, toluene–diethyl ether, (40 : 1)] afforded the desired product (5.0 mg, 42%). A ^{1}H NMR spectrum was recorded, but the complexity due to the mixture of regioisomers prevented a complete interpretation. LD-MS obsd (POPOP) 5155.7 [M^+], 5080.8 [M^+ − SAc], 4980.6, 4267.7 [M^+ − (*t*-Bu$_4$Pc)Eu]; calcd exact mass 5154.73 ($C_{308}H_{258}CeEu_3N_{36}O_2S_2$); λ_{abs} 348, 421, 493, 525, 617, 729 nm.

Electrochemical studies

The solution electrochemical studies were performed using techniques and instrumentation previously described.[45] For all triple deckers and dyads, the solvent was dried distilled CH_2Cl_2 and 0.1 M Bu_4NPF_6 (Aldrich, recrystallized three times from methanol and dried under vacuum at 110 °C) served as supporting electrolyte. The potentials were measured *vs.* Ag/Ag^+; $E_{1/2}(FeCp_2/FeCp_2^+)$ = 0.19 V. The scan rate was 0.1 V s^{-1}. All CH_2Cl_2 used in the following procedure also was dried and distilled.

Cyclic voltammograms of the SAMs were recorded with an Ensman Instruments 400 potentiostat. These electrochemical studies utilized a 75 μm Au microband working electrode that was formed on a borosilicate glass microscope slide (Fisher, Fair Lawn, NJ) by vapor deposition of 99.99% gold (1 Oz. Canadian Maple Leaf, obtained locally) in a CHA SE-600 4-pocket E-beam evaporator (CHA Industries, Menlo Park, CA). The microscope slides are first cleaned by boiling in piranha solution (30% H_2O_2–10% solution, 70% H_2SO_4) for 20 min, rinsed with deionized water and dried in a vacuum oven at 100 °C. A shadow mask is used to allow deposition of 2000 Å of Au (utilizing a 100 Å Cr underlayer to promote adhesion) to form the electrode (four Au microbands per slide, each 75 μm wide) with a contact pad at the edge of the glass slide.

The electrochemical cell was defined by placing a patterned 2 mm thick sheet of polymerized polydimethylsiloxane (PDMS) to frame a ∼12 mm^2 circular area over the Au microband electrode. PDMS adheres well to glass surfaces and prevents leakage of solution, thereby defining the area of electrode that will be exposed to electrolyte solution. This defines a ∼3000 μm^2 Au microband electrode. The PDMS well

was filled with a 2 mg mL^{-1} solution of the dyad in CH_2Cl_2 containing 1 drop of ethanol and sonicated for 10 min. After sonication, the solution along with the well was removed from the slide. The slide was copiously rinsed with CH_2Cl_2 and dried in a stream of N_2. A fresh PDMS well was placed around the working electrode, filled with electrolyte (CH_2Cl_2 containing 1.0 M Bu_4NPF_6), and the Ag counter and Pt reference electrodes were inserted into the solution. The potentials were measured *vs.* Ag/Ag^+; $E_{1/2}(FeCp_2/FeCp_2^+) = 0.19$ V. The scan rate was 100 V s^{-1}.

The molecular area of each dyad SAM was determined by integrating the charge under an oxidation wave that corresponded to a one-electron event. The electrochemical surface area was evaluated by measuring the peak current resulting from the oxidation of 1 mM ferrocene and applying the Randle–Sevcik equation.[46] In this measurement, the SAM was first stripped from the surface by scanning to high potential; the solution and electrolyte were removed from the cell and the cell was rinsed. A solution containing the ferrocene was then added and a voltammogram recorded.

Acknowledgements

This work was supported by the DARPA Moletronics Programs, administered by the ONR (MDA-972-01-C-0072), and by ZettaCore, Inc. Mass spectra were obtained at the Mass Spectrometry Laboratory for Biotechnology at North Carolina State University. Partial funding for the facility was obtained from the North Carolina Biotechnology Center and the NSF.

References

1 K. M. Roth, N. Dontha, R. B. Dabke, D. T. Gryko, C. Clausen, J. S. Lindsey, D. F. Bocian and W. G. Kuhr, *J. Vac. Sci. Technol. B*, 2000, **18**, 2359.
2 D. T. Gryko, C. Clausen, K. M. Roth, N. Dontha, D. F. Bocian, W. G. Kuhr and J. S. Lindsey, *J. Org. Chem.*, 2000, **65**, 7345.
3 C. Clausen, D. T. Gryko, R. B. Dabke, N. Dontha, D. F. Bocian, W. G. Kuhr and J. S. Lindsey, *J. Org. Chem.*, 2000, **65**, 7363.
4 C. Clausen, D. T. Gryko, A. A. Yasseri, J. R. Diers, D. F. Bocian, W. G. Kuhr and J. S. Lindsey, *J. Org. Chem.*, 2000, **65**, 7371.
5 D. T. Gryko, F. Zhao, A. A. Yasseri, K. M. Roth, D. F. Bocian, W. G. Kuhr and J. S. Lindsey, *J. Org. Chem.*, 2000, **65**, 7356.
6 J. Li, D. Gryko, R. B. Dabke, J. R. Diers, D. F. Bocian, W. G. Kuhr and J. S. Lindsey, *J. Org. Chem.*, 2000, **65**, 7379.
7 D. Gryko, J. Li, J. R. Diers, K. M. Roth, D. F. Bocian, W. G. Kuhr and J. S. Lindsey, *J. Mater. Chem.*, 2001, **11**, 1162.
8 J. W. Buchler and D. K. P. Ng, in *The Porphyrin Handbook*, eds. K. M. Kadish, K. M. Smith and R. Guilard, Academic Press, San Diego, CA, 2000, Vol. 3, pp. 245–294.
9 J. Jiang, W. Liu, W.-F. Law and D. K. P. Ng, *Inorg. Chim. Acta*, 1998, **268**, 49.
10 M. Ruben, E. Breuning, J.-P. Gisselbrecht and J.-M. Lehn, *Angew. Chem., Int. Ed.*, 2000, **39**, 4139.
11 C. B. Gorman, *Adv. Mater.*, 1997, **9**, 1117.
12 In the electrical engineering literature, a 'multistate counter' of the type we describe would more appropriately be referred to as an integrator owing to the different potential that accompanies each distinct state. By contrast, in a true counter, successive digits are accessed by application of the same potential. We have elected to use the term 'multistate counter' herein owing to the simple correspondence of distinct oxidation states and counting level.
13 D. Chabach, A. De Cian, J. Fischer, R. Weiss and M. E. M. Bibout, *Angew. Chem., Int. Ed. Engl.*, 1996, **35**, 898.
14 T. Gross, F. Chevalier and J. S. Lindsey, *Inorg. Chem.*, 2001, **40**, 4762.
15 The term Por or Pc refers generically to the dianion of a free base porphyrin or free base phthalocyanine, respectively.
16 Each europium double decker is assumed to be a radical species.
17 C.-P. Wong, R. F. Venteicher and W. D. Horrocks Jr., *J. Am. Chem. Soc.*, 1974, **96**, 7149.
18 M. Sommerauer, C. Rager and M. Hanack, *J. Am. Chem. Soc.*, 1996, **118**, 10085.
19 J. K. Duchowski and D. F. Bocian, *J. Am. Chem. Soc.*, 1990, **112**, 8807.
20 J. S. Lindsey, in *The Porphyrin Handbook*, eds. K. M. Kadish, K. M. Smith and R. Guilard, Academic Press, San Diego, CA, 2000, Vol. 1, pp. 45–118.
21 The *meso*-substituted metalloporphyrins have the following symmetry point groups: A_4 porphyrin (D_{4h}); A_3B porphyrin (C_{2v}); *cis*-A_2B_2 porphyrin (C_{2v}); *trans*-A_2B_2 porphyrin (D_{2h}); *trans*-A_2BC porphyrin (C_{2v}); *cis*-A_2BC porphyrin (C_s); ABCD porphyrin (C_s). Only the latter two types of substituted porphyrins have no mirror plane perpendicular to the plane of the macrocycle.
22 This analysis assumes that (a) the Por and/or Pc components that complete the triple decker themselves have mirror planes perpendicular to the plane of the macrocycle, and (b) rotation about the cylindrical axis of the triple decker is unhindered.
23 This analysis describes the minimum number of structural isomers that can result for each triple decker and for each type of dyad. In practice, each triple decker described herein incorporates one or two tetra-*tert*-butylphthalocyanine units; accordingly, each triple decker exists as a mixture of diastereomers. The presence of the diastereomers stems from the fact that the tetra-*tert*-butylphthalocyanine employed in these reactions is comprised of four regioisomers. Thus, those triple deckers that incorporate a *cis*-A_2BC porphyrin afford a mixture of diastereomers rather than a mere pair of enantiomers due to the presence of one or two tetra-*tert*-butylphthalocyanine units in the triple decker. It follows that each dyad that incorporates one or more tetra-*tert*-butylphthalocyanine ligands also exists as a mixture of diastereomers. However, the presence of *syn versus anti* isomers is expected to pose more distinct spatial requirements upon surface binding of a horizontal dyad than the existence of diastereomers due to the presence of multiple tetra-*tert*-butylphthalocyanine units.
24 P. D. Rao, S. Dhanalekshmi, B. J. Littler and J. S. Lindsey, *J. Org. Chem.*, 2000, **65**, 7323.
25 B. J. Littler, M. A. Miller, C.-H. Hung, R. W. Wagner, D. F. O'Shea, P. D. Boyle and J. S. Lindsey, *J. Org. Chem.*, 1999, **64**, 1391.
26 W.-S. Cho, H.-J. Kim, B. J. Littler, M. A. Miller, C.-H. Lee and J. S. Lindsey, *J. Org. Chem.*, 1999, **64**, 7890.
27 P. D. Rao, B. J. Littler, G. R. Geier III and J. S. Lindsey, *J. Org. Chem.*, 2000, **65**, 1084.
28 D. Gryko and J. S. Lindsey, *J. Org. Chem.*, 2000, **65**, 2249.
29 D. Battisti, L. Tomilova and R. Aroca, *Chem. Mater.*, 1992, **4**, 1323.
30 The relative distribution of the four isomers of each tetra-*tert*-butylphthalocyanine ligand in the triple deckers is not known. However, the complexity of the ^1H NMR spectra is consistent with the presence of tetra-*tert*-butylphthalocyanine isomers in the triple deckers.
31 R. W. Wagner, Y. Ciringh, C. Clausen and J. S. Lindsey, *Chem. Mater.*, 1999, **11**, 2974.
32 Analytical SEC data are uncorrected.
33 R. P. Hsung, J. R. Babcock, C. E. D. Chidsey and L. R. Sita, *Tetrahedron Lett.*, 1995, **26**, 4525.
34 A. V. Rukavishnikov, A. Phadke, M. D. Lee, D. H. LaMunyon, P. A. Petukhov and J. F. W. Keana, *Tetrahedron Lett.*, 1999, **40**, 6353.
35 D. K. P. Ng and J. Jiang, *Chem. Soc. Rev.*, 1997, **26**, 433.
36 J. Jiang, R. L. C. Lau, T. W. D. Chan, T. C. W. Mak and D. K. P. Ng, *Inorg. Chim. Acta*, 1997, **255**, 59.
37 M. Moussavi, A. De Cian, J. Fischer and R. Weiss, *Inorg. Chem.*, 1986, **25**, 2107.
38 D. Chabach, M. Lachkar, A. De Cian, J. Fischer and R. Weiss, *New J. Chem.*, 1992, **16**, 431.
39 T.-H. Tran-Thi, T. A. Mattioli, D. Chabach, A. De Cian and R. Weiss, *J. Phys. Chem.*, 1994, **98**, 8279.
40 W. Liu, J. Jiang, N. Pan and D. P. Arnold, *Inorg. Chim. Acta*, 2000, **310**, 140.
41 J. W. Buchler, A. De Cian, J. Fischer, M. Kihn-Botulinski, H. Paulus and R. Weiss, *J. Am. Chem. Soc.*, 1986, **108**, 3652.
42 S. E. Creager and G. K. Rowe, *J. Electroanal. Chem.*, 1994, **370**, 203.
43 (*a*) D. Fenyo, B. T. Chait, T. E. Johnson and J. S. Lindsey, *J. Porphyrins Phthalocyanines*, 1997, **1**, 93; (*b*) N. Srinivasan, C. A. Haney, J. S. Lindsey, W. Zhang and B. T. Chait, *J. Porphyrins Phthalocyanines*, 1999, **3**, 283.
44 R. W. Wagner, T. E. Johnson and J. S. Lindsey, *J. Am. Chem. Soc.*, 1996, **118**, 11166.
45 J. Seth, V. Palaniappan, R. W. Wagner, T. E. Johnson, J. S. Lindsey and D. F. Bocian, *J. Am. Chem. Soc.*, 1996, **118**, 11194.
46 A. J. Bard and L. R. Faulkner, *Electrochemical Methods: Fundamentals and Applications*, Wiley, New York, 1980.